Chapter Four

Seismic Impacts Resulting from Well Stimulation

Bill Foxall, Nathaniel James Lindsey, Corinne Bachmann[1]

[1] *Lawrence Berkeley National Laboratory, Berkeley, CA*

4.1. Abstract

Induced seismicity refers to seismic events caused by human activities. These activities include injection of fluids into the subsurface, when elevated fluid pore pressures can lower the frictional strengths of faults and fractures leading to seismic rupture. The vast majority of induced earthquakes that have been attributed to fluid injection were too small to be perceptible by humans. However, events induced by injection have on several occasions been felt at the ground surface, and in extremely rare cases have produced ground shaking large enough to cause damage. These larger events can occur when large volumes of water are injected over long time periods (months to years) into zones in or near potentially active earthquake sources.

The relatively small fluid volumes and short time durations (hours) involved in most hydraulic fracturing operations are generally not sufficient to create pore-pressure perturbations of large enough spatial extent to generate induced seismicity of concern. Current hydraulic fracturing activity is not considered to pose a significant seismic hazard in California. To date, only one felt earthquake attributed to hydraulic fracturing in a California oil or gas field has been documented, and that was anomalous because it was a slow-slip event that radiated much lower energy at much lower dominant frequencies than ordinary earthquakes of similar size.

In contrast to hydraulic fracturing, earthquakes as large as magnitude 5.7 have been linked to injection of large volumes of wastewater into deep disposal wells in the eastern and central United States. Compared to states that have recently experienced large increases in induced seismicity, water volumes disposed per well in California are relatively small.

Despite decades of production and injection in oil and gas fields, extensive seismic monitoring, and vigorous seismological research in California, there are no published reports of induced seismicity associated with wastewater disposal related to oil and gas operations in the state. However, the potential seismic hazard posed by current water

disposal in California is uncertain because possible relationships between seismicity and wastewater injection have yet to be studied in detail. Injection of larger volumes of produced water from increased well stimulation activity and the subsequent increase in oil and gas production could conceivably increase the hazard. Given the active tectonic setting of California, it would be prudent to carry out assessments of induced seismic hazard and risk for future injection projects, based on a comprehensive study of spatial and temporal relationships between wastewater injection and seismicity.

The closest wastewater disposal wells to the San Andreas Fault (SAF) are located in oilfields just over 10 km (6.2 mi) away in the southern San Joaquin Valley. It is unlikely that current wastewater injection in these wells would induce earthquakes on the fault. If in the future significantly higher-volume injection were to take place in or close to these existing oilfields, then it is plausible that the likelihood of inducing earthquakes on the SAF could increase.

The probability of inducing larger, hazardous earthquakes by wastewater disposal could likely be reduced by following protocols similar to those that have been developed for other types of injection operations, such as enhanced geothermal. Even though hydraulic fracturing itself rarely induces felt earthquakes, application of similar protocols could protect against potential worst-case outcomes resulting from these operations as well.

4.2. Introduction

Induced seismicity refers to seismic events caused by human activities, which can include injection of fluids into the subsurface. The vast majority of induced earthquakes that have been attributed to fluid injection were too small to be perceptible by humans. However, seismic events induced by fluid injection have on several occasions been felt at the ground surface, and in extremely rare cases have produced ground shaking large enough to cause damage. This chapter reviews the current state of knowledge about induced seismicity, and discusses the data and research that would be required to determine the potential for induced seismicity in California, including along the SAF. Measures to assess and, if necessary, to reduce the risk from induced seismicity are also discussed.

4.2.1. Chapter Structure

This introductory section provides a brief overview of the general characteristics of earthquakes and the basic cause of earthquakes induced by subsurface fluid injection, followed by a summary of observed cases of induced seismicity related to well stimulation activities. Section 4.3 first discusses the potential impacts of induced seismicity in terms of the risks of nuisance and structural damage caused by ground shaking, and then describes the mechanics of fluid-induced earthquakes and the characteristics of seismicity sequences related to well stimulation. Section 4.4 considers factors that could influence the potential for well stimulation in California to induce seismicity, and describes the studies needed to assess that potential. Suggested measures to lower the likelihood of induced earthquakes

occurring and hence reduce the risks are described in Section 4.5. Section 4.6 identifies gaps in the available data that presently limit our ability to evaluate induced seismicity in California, and then discusses potential actions to address those gaps. A summary of findings and conclusions are presented in Sections 4.7 and 4.8, respectively.

4.2.2. Natural and Induced Earthquakes

An earthquake is a seismic event that involves sudden slippage along an approximately planar fault or fracture in the Earth. This process occurs naturally as a result of stresses that build up owing to deformation within the Earth's crust and interior. The size of an earthquake depends primarily on the area of the patch on the fault that slips and the amount of relative displacement across the slip patch. Earthquake sizes range over many orders of magnitude. There are many more small events than large events; a decrease of one unit in the magnitude scale (see below and Appendix 4.A) corresponds roughly to a ten-fold increase in the number of events. As a result, the vast majority of earthquakes can only be detected by sensitive instruments. If, however, the slip area is sufficient to generate an earthquake larger than magnitude 2 to 3, the energy released during the event can generate seismic waves sufficient to produce ground motions that can be felt by humans, and larger events (usually about magnitude 5 and above) can in some cases cause structural damage. Over one million natural earthquakes of magnitude 2 or more occur worldwide every year (National Research Council (NRC), 2013).

As discussed in Appendix 4.A, several alternative magnitude scales are commonly used to express earthquake sizes. These employ different methods to compute magnitude, but all of the scales are roughly consistent with each other (within one-half magnitude unit) for earthquakes smaller than about magnitude 7. Henceforth in this report, we use published moment magnitudes, M_w. When discussing specific earthquakes for which M_w was not reported, we use the published magnitude, which, for the earthquakes discussed below, include only local magnitude, M_L and body-wave magnitude, m_b. In published cases when the scale was not specified, or to refer to magnitude in a general sense, we use the designation "M". Definition of the term "microseismicity" is somewhat arbitrary; for example, in earthquake seismology microseismicity usually refers to earthquakes smaller than M_w2-3, whereas in hydrofracture monitoring it commonly refers to events smaller than M_w0. In this report, we use microseismicity to describe earthquakes having magnitudes less than M_w3.

Earthquakes caused by human activity are termed *induced seismicity*. Activities that can induce earthquakes include underground mining, reservoir impoundment, and the injection and withdrawal of fluids as part of energy production activities (NRC, 2013). Note that some authors distinguish between "induced" and "triggered" events according to various criteria (e.g., McGarr et al., 2002; Baisch et al., 2009). In this report we do not make this distinction, but refer to all earthquakes that occur as a consequence of human activities as induced seismicity.

4.2.3. Induced Seismicity Related to Well Stimulation

Induced earthquakes related to well stimulation can be caused by injection of fluids into the subsurface, both for hydraulic fracturing stimulation itself and for disposal of recovered fluids and produced wastewater during stimulation and subsequent production. The predominant mechanism responsible for a fluid injection-induced earthquake is an increase in the pore-fluid pressure within a fault that reduces the confining stress that holds the two sides of the fault together, thus reducing its frictional resistance to slip (Hubbert and Rubey, 1959). Applying this mechanism to estimate the probability that seismic events of concern will be caused by a particular operation requires measurement or calculation of (1) the development of the subsurface pore-pressure perturbation in time and space, (2) characterization of faults likely to experience elevated pressures, and (3) characterization of rock material properties and *in situ* stress conditions. Because in practice these input parameters are often known only within broad bounds, an important part of the analysis is to properly constrain the uncertainties in order to correctly determine uncertainty bounds on the calculated event probabilities.

To date, the largest observed event attributed to hydraulic-fracture well stimulation is an M_L3.8 earthquake that occurred in the Horn River Basin, British Columbia, in 2011 (BC Oil and Gas Commission, 2012). The generally lower magnitudes of events associated with hydraulic fracturing relative to those induced by wastewater disposal are usually attributed to the short durations, smaller volumes, and flowback of injection fluids following stimulation, which result in smaller regions affected by elevated fluid pressures compared with the longer time periods and much higher volumes of wastewater injection. None of the events related to hydraulic fracturing reported in the literature have occurred in California and (with the possible exception of one paper that discusses an abnormal slow earthquake) we have found no published study that addressed this topic in California. If hydraulic fracturing operations carried out in California to date have, in fact, not induced normal seismic events above M2, possible explanations are that most of the well stimulation takes place in vertical wells at relatively shallow injection depths and employs relatively small injected volumes (Chapter 2). Volume I of this report concludes that salient features of hydraulic fracturing in California in the near- to mid-term are expected to be similar to those experienced thus far. If in the longer term hydraulic fracturing in the state shifts to larger injected volumes and deeper stimulation, then the likelihood of induced seismicity from hydrofracturing could increase.

The largest observed earthquake suspected to be related to wastewater disposal in the U.S. to date is a 2011 M_w5.7 event near Prague, Oklahoma (Keranen et al., 2013; Sumy et al., 2014), although the cause of this event is still under debate (Keller and Holland, 2013; McGarr, 2014). The largest earthquake clearly linked to stimulation-related wastewater injection is a 2011 M_w5.3 event in the Raton Basin of Colorado and New Mexico (Rubinstein et al., 2014). Despite decades of oil and gas production and wastewater injection, extensive seismic monitoring and exceptional in-depth research into

the occurrence and mechanics of regional and local earthquakes, there are no published reports of induced seismicity caused by wastewater disposal related to oil and gas operations in California. However, there has been no comprehensive, in-depth study of the relationship between seismicity and disposal operations in the state.

Typical wastewater volumes injected per well in California are generally less than those associated with well stimulation operations in other parts of the country where induced seismicity has occurred. For example, typical wastewater volumes injected in Kern County to date have been about one fourth of those resulting from well stimulation in the Barnett shale and injected in the Dallas-Fort Worth area in Texas, where induced seismicity has been reported from ongoing observational studies. This might suggest that at the present time the potential for induced seismicity related to wastewater disposal in California may be relatively low compared with some other regions in the U.S. However, because the possible relationship between injection and seismicity in California has yet to be investigated, the potential seismic impact is at present unknown. Expanded well stimulation activity would require disposal of larger volumes of fluid, which would potentially increase the impact. Given the active tectonic setting of California, it will be prudent to carry out an assessment of induced seismic hazard and risk as part of the permitting process for future injection projects, particularly in areas where there are active faults and that experience naturally occurring seismicity. A comprehensive study of spatial and temporal relationships between wastewater injection and seismicity is necessary to provide a basis for such assessments. The chance of inducing larger, hazardous earthquakes would most likely be reduced by following protocols similar to those that have been developed for other types of injection operations, such as those for enhanced geothermal energy production (e.g. Majer et al., 2012).

4.3. Potential Impacts of Induced Seismicity

Induced seismicity can produce felt or even damaging ground motions when large volumes of water are injected over long time periods into zones in or near potentially active earthquake sources. The relatively small fluid volumes and short time durations involved in most hydraulic fracturing operations themselves are generally not sufficient to create pore-pressure perturbations of large enough spatial extent to generate induced seismicity of concern. In contrast, earthquakes as large as M_w5.7 have been linked to injection of large volumes of wastewater into deep disposal wells in the eastern and central United States (Keranen et al., 2013; Sumy et al., 2014).

Seismic hazard is defined as the probability that a specific level of ground shaking will occur at a particular location during in a specified interval of time. This formal definition is a departure from the meaning of the more general term “hazard”, which refers to possible negative outcomes or impacts. In this chapter, the word hazard alone indicates the more general possibility of impact, while the term *seismic hazard* will be used to refer to the formal definition used by the seismic hazard community. *Seismic risk* is the probability of a consequence, such as deaths and injuries or a particular degree of building damage, resulting from the shaking. Risk, as defined with regard to seismic ground

motion, therefore combines the seismic hazard with the vulnerability of the population and built infrastructure to shaking, so that for the same seismic hazard, the risk is higher in densely populated areas. This use of the word risk is consistent with that used in other fields and involves both likelihood (probability of occurrence) and impact severity.

4.3.1. Building and Infrastructure Damage

Conventional seismic hazard and risk assessment deal with building and infrastructure damage—and the possible resulting injuries and loss of life—caused by strong ground shaking generated by naturally occurring earthquakes. The threshold magnitude for earthquakes to be capable of causing structural damage is generally considered to be about M_w5. Ground shaking from induced seismicity poses a potential incremental hazard above the natural background that needs to be considered in assessing the overall risk of an injection operation.

4.3.2. Nuisance from Seismic Ground Motion and Public Perception

Unlike assessing risk from naturally occurring seismicity, in the case of induced seismicity the likelihood of causing public nuisance from small events that are felt in nearby communities also has to be considered. This seismic risk includes minor cosmetic damage such as cracked plaster, as well as annoyance, alarm, and other adverse effects such as disrupted sleep. The magnitude threshold for felt events can be as low as M1.5–2.0 for the shallow depths of seismicity that are typically associated with fluid injection. In general, small earthquakes occur more frequently than large ones (see Section 4.2.2). Therefore, the frequency of occurrence of felt events can be relatively high, so that they may pose an ongoing impact on the quality of life in nearby communities.

4.3.3. Mechanics of Earthquakes Induced by Subsurface Fluid Injection

This section summarizes the physical mechanisms responsible for earthquakes induced by fluid injection. Fluid injection related to well stimulation takes place both for hydraulic fracturing and for wastewater disposal. In general, induced seismicity related to well stimulation is dominated by perturbations in fluid pore pressure, rather than by changes in *in situ* principal stresses (NRC, 2013). The characteristics of pore-pressure perturbations and induced seismicity resulting from hydraulic fracturing and wastewater disposal and their potential impacts are discussed in Sections 4.3.4 and 4.3.5, respectively.

During fluid injection there can be two types of rock failure, tensile and shear. Below we describe these two types of failure in the context of injection operations related to well stimulation.

4.3.3.1. Tensile Fracturing

The primary objective of hydraulic fracturing is to inject fluid into the earth to create a new fracture that connects the pores and existing fractures in the surrounding rock with the well, thus forming a permeable pathway that enables the oil and/or gas (and water) in the pores and fractures to be recovered. Hydraulic fractures are created by the rock failing in tension when the fluid pressure exceeds the *in situ* minimum principal stress (see Appendix 4.B). In this type of failure, a roughly planar fracture forms in the rock, and the walls of the fracture move apart perpendicular to the fracture plane at the same time as the fracture propagates (grows) at the crack tip in the direction parallel to the fracture plane. While there may be bursts of fracturing over short length scales at the crack tip, large-scale hydraulic fractures form slowly (hours) and can extend up to hundreds of meters away from the well. Although the physical processes at the crack tip are not yet fully understood, it appears that the amount of seismic energy radiated as the tensile fracture propagates is small and difficult to detect. Therefore, hydraulic fracture growth itself is responsible for little, if any, of the seismicity recorded in the field, and it probably makes little or no contribution to seismic hazard.

4.3.3.2. Shear Failure on Pre-existing Faults and Fractures

Shear failure on existing faults and fractures can occur both during stimulation by hydraulic fracturing and during wastewater disposal. During stimulation, shear events serve to enhance the permeability of small, existing fractures and faults and to link them up to create conductive networks connected to the main hydraulic fracture. Shear slip is the type of failure that occurs in most natural tectonic earthquakes, and it is shear events on larger faults that can produce perceptible or damaging ground motions at the Earth's surface.

During a shear event the two faces of the fault slip in opposite directions to each other parallel to the fault surface. The conditions for the initiation of shear slip are governed by the balance between the shear stress applied parallel to the fault surface, the cohesion across the fault, and the frictional resistance to sliding (shear strength). Assuming that the cohesion is negligible, these conditions are summarized in the Coulomb criterion,

$$\tau = \mu\,(\sigma - p) \qquad (4\text{-}1)$$

in which an applied shear stress (τ) is balanced by the shear strength, which is the product of the coefficient of friction (μ) and the difference between normal stress (σ) and pore-fluid pressure (p). Shear stress is directed along the fault plane, while normal stress is directed perpendicular to the plane. The quantity (σ - p) is called the effective stress. Effective stress represents the difference between the normal stress, which pushes the two sides of the fault together and increases the frictional strength, and the fluid pressure within the fault, which has the opposite effect. The Coulomb criterion states that slip will occur when the shear stress (τ) exceeds the strength of the fracture (right-hand

side of Equation 4-1). The shear stress that drives earthquake slip results from strain that accumulates in the Earth's crust, primarily as a result of tectonic and gravitational loading. An earthquake occurs when a fault fails in shear, releasing stored strain energy. In a tectonic earthquake, fault failure occurs when the accumulated shear stress reaches the critical value. Fault failure can also be initiated by decreasing the effective stress either by decreasing the normal stress (σ) that holds the fault closed and unable to slip, or by increasing the fluid pressure, which tends to push the sides of the fault apart, enabling slip.

4.3.3.3. Factors Influencing the Probability of Occurrence of Induced Earthquakes

If elevated pore pressures produced by either hydraulic fracturing or wastewater injection reach nearby faults or fractures, the resulting decrease in effective stress on the fault/fracture planes can cause induced seismicity. Therefore, in both activities, one consideration in developing an injection strategy should be to prevent the pressure perturbation from reaching larger faults capable of generating significant seismic events. This would help to minimize the seismic hazard and, in the case of well stimulation, to inhibit the fracture from propagating beyond the bounds of the hydrocarbon reservoir and providing a potential leakage pathway.

The primary factors that determine the probability of inducing seismic events are the volume of injected fluids, the spatial extent of the affected subsurface volume, ambient stress conditions, and the presence of faults that are well oriented for slip and are near-critically stressed (Appendix 4.B). The primary factors affecting the magnitude and extent, shape, and orientation of a pore-pressure perturbation include the injection rate and pressure, which are generally interdependent, the total volume injected, the hydraulic diffusivity (a measure of how fast a pore-pressure perturbation propagates in the fluids in the pore space), and the stress state and natural fracture orientation and conductivity under injection conditions. At early stages of an injection, the extent of the pressure perturbation depends on the hydraulic diffusivity and the duration of the injection, while the maximum pore pressure depends on the product of injection rate and duration divided by the permeability (NRC, 2013). At later stages, the induced pore-pressure field does not depend on the injection rate or permeability, but becomes proportional to the total volume of fluid injected.

4.3.3.4. Maximum Magnitude of Induced Earthquakes

The vast majority of earthquakes induced by fluid injection in general do not exceed M1 (e.g., Davies et al., 2013; Ellsworth, 2013). However, larger magnitude earthquakes ($M > 2$) have resulted from both wastewater injection and hydraulic fracturing. McGarr (2014) proposed estimating upper bounds on induced earthquake magnitudes based on net total injected fluid volume, observing that such a relationship is found to be valid for the largest induced earthquakes that have been attributed to fluid injection. Shapiro et al. (2011) proposed a similar approach to estimating maximum magnitude, based on the dimensions of the overpressurized zone deduced from observed microseismicity. Brodsky and Lajoie

(2013) also concluded that induced seismicity rates associated with the Salton Sea geothermal field correlate with net injected volume. However, the approaches proposed by both McGarr (2014) and Shapiro et al. (2011) appear to imply that fault rupture induced by the injection occurs only within the volume of pore-pressure increase. An alternative hypothesis is that a rupture that initiates on a fault patch within the overpressured volume can continue to propagate beyond its boundaries, in which case the possible maximum magnitude is determined by the size of the entire fault. Indeed, McGarr (2014) does not regard that his relationship determines an absolute physical limit on event size.

4.3.4. Induced Seismicity Resulting from Hydraulic Fracturing Operations

Because hydraulic fracture treatments are carried with relatively small injected volumes over short time periods and a proportion of the fluid flows back up the well following stimulation, the volume of the subsurface affected by pressure perturbations is usually confined within a few hundred meters of the wellbore, as shown by microseismic and tiltmeter fracture mapping results (e.g., Shemeta et al., 1994; Shapiro and Dinske, 2009; Davies et al., 2012; Fisher et al., 2002; Fisher et al., 2004). Davies et al. (2013) cite evidence to suggest that induced shear events in the vicinities of stimulation zones are mainly caused by fluids leaking off into preexisting faults and fractures intersected by the hydraulic fracture. Shear failure may also occur on nearby, favorably oriented faults and fractures isolated from the zone of increased pressure due to perturbation of the local stress field near the tip of the propagating hydraulic fracture (e.g., Rutledge and Phillips, 2003).

There can be a time delay between the beginning of injection and the occurrence of larger ($M > 2$) events, and in several cases the largest event has occurred after injection ceases. The longest time delay observed to date following a well stimulation injection was almost 24 hours before the occurrence of the largest (M_L3.8) event at the Horn River Basin, BC site (BC Oil and Gas Commission, 2012). A 2011 M_L2.3 earthquake in Blackpool, UK, occurred about 10 hours after injection ceased at the Preese Hall 1 stimulation well (de Pater and Baisch, 2011).

Overall, because of the relatively small volumes of rock that experience elevated pressures, there is a lower potential seismic hazard from short-duration hydraulic fracture operations than from disposal of large volumes of wastewater. The fact that, to date, the maximum magnitudes of events caused by hydraulic fracturing have been well below those usually considered to be capable of causing damage suggests that the likelihood of damaging events being induced by hydraulic fracturing is very low.

Published cases of known or suspected fluid injection-induced seismicity resulting from well stimulation and wastewater disposal that included events greater than M1.5 are described in Appendix 4.C. Five out of the six seismicity sequences listed in Table 4.C-1 attributed to hydraulic fracturing worldwide included felt earthquakes, and in all but one of these five cases, only one or two events were reported felt. This suggests that the risk of nuisance is also quite low. However, it is pertinent that all but one of the cases involving

felt earthquakes have occurred during the major upsurge in well stimulation activity since 2010, so that a further increase in activity in a particular region may increase the overall seismic hazard and risk there beyond past experience.

4.3.5. Induced Seismicity Resulting from Wastewater Disposal

Large-scale, continuous injection of wastewater into a single formation over time periods of months to years commonly generates overpressure fields of much larger extent than those resulting from well stimulation. For example, at the Rocky Mountain Arsenal, Colorado significant earthquakes caused by fluid injection occurred 10 km (6.2 mi) away from the injection well (Healy et al., 1968; Herrmann et al., 1981; Nicholson and Wesson, 1990). Hydrologic modeling of injection into the deep well at the site indicated that the seismicity tracked a critical pressure surface of 3.2 MPa (Hsieh and Bredehoeft, 1981). Long time delays between the cessation of injection and the occurrence of larger events have also been observed in several cases. For example, at the Rocky Mountain Arsenal, the largest earthquake (M_w4.8) occurred 17 months after injection ceased (Herrmann et al., 1981).

Generally, the likelihood of inducing larger events increases as the volume of injected wastewater increases. The largest earthquake suspected of being related to wastewater disposal is the 2011 M_w5.7 Prague, Oklahoma event (Keranen et al., 2013; Sumy et al., 2014), but the causal mechanism of this event is still the subject of active research, and the possibility that it was a natural tectonic earthquake cannot confidently be ruled out at present. The largest earthquake for which there is clear evidence for a causative link to stimulation-related wastewater injection is the 2011 M_w5.3 event in the Raton Basin of Colorado and New Mexico (Rubinstein et al., 2014). It is important to note, however, that significant induced seismicity has occurred at very few of the tens of thousands of wastewater disposal wells currently or formerly active in the U.S. (e.g., NRC, 2013; Ellsworth, 2013; Weingarten and Ge, 2014).

In most of the reported cases of induced seismicity associated with wastewater disposal listed in Table 4.C-1, events occurred both in the sedimentary formation into which the injection took place and, except in the Dallas-Fort Worth and Cleburne, Texas sequences, in the underlying crystalline basement rocks. In all of the cases, the seismicity illuminated planar features that were interpreted as favorably oriented faults reactivated by injection. Most of the faults interpreted from the seismicity had not been mapped on the ground surface. Reactivation of faults well below the injection interval can occur if there is hydraulic communication between them and the well (Horton, 2012; Justinic et al., 2013), and although the matrix permeability of basement rock is generally very low, critically stressed faults and fractures in this part of the brittle crust can serve as high permeability channels (Townend and Zoback, 2000; Fehler et al., 1998; Shapiro et al., 2003). The maximum depth of seismicity in the cases listed in Table 4.C-1 ranged from about 4 to 8 km (2.5 to 5 mi).

All seven of the M4 and larger earthquakes that occurred within the fluid injection-induced seismicity sequences listed in Table 4C-1 and that have relatively accurate hypocentral locations constrained by local seismic networks nucleated at depths between 3 and 6 km (1.9 and 3.7 mi). This depth range is assumed to correspond to the zone some distance below the injection interval where high fluid overpressures over relatively large fault areas coincide with stresses that put favorably oriented faults into a near-critical state; i.e. where the pressure reaches the critical value needed to nucleate a larger event. Deeper seismicity corresponds both to aftershocks of the larger events and to smaller magnitude events perhaps triggered at lower pressures.

Relatively high seismic hazard from earthquakes below M_w4.5 translates into a greater risk of nuisance if the seismicity occurs close to inhabited areas. Of the 14 events in Table 4.C-1 attributed to wastewater disposal, five were larger than M_w4.5. Only three of these, the M_w4.8 1967 Rocky Mountain Arsenal, the M_w5.7 2011 Prague, and the M_w5.3 2011 Raton Basin events, caused anything more significant than localized minor damage. However, as noted above, events as small as about M_w5 are generally considered to be capable of causing significant damage under certain circumstances (shallow focal depth, construction that is not seismically resistant, etc.), at least in the vicinity of the epicenter. Therefore, although it may be low in absolute terms, the seismic risk of damage associated with wastewater injection is relatively much greater than that associated with well stimulation. In view of the dramatic increase in seismicity—including all but one of the events greater than M_w4.5 in Table 4.C-1—that has accompanied the upswing in wastewater disposal in some parts of the U.S. beginning in 2010 (see U.S. Geological Survey, 2015), a future increase in the rate of operations in a particular region may increase the likelihood of damage there, as well as nuisance.

4.4. Potential for Induced Seismicity in California

All of the U.S. cases of induced seismicity related to fluid injection discussed in Appendix 4.C occurred within the continental interior, where tectonic deformation rates are very low. California, on the other hand, is situated within an active tectonic plate margin, where the rapid buildup of shear stress on the numerous active faults (Figure 4.4-1) results in much higher seismicity rates in many areas of the state than in the continental interior, as can be seen in Figure 4.4-2. If, as discussed in Appendix 4.B, the Earth's upper crust is generally in a near-critical stress state, then the high loading rates would imply that a relatively high proportion of faults in California will be close to failure at any given time, and hence susceptible to earthquakes triggered by small effective stress or shear stress perturbations.

4.4.1. California Faults and Stress Field

Unlike the central and eastern U.S., a large number of active faults have been mapped at the Earth's surface and characterized in California. Figures 4.4-1 and 4.4-2 show the surface traces of active faults in central and southern California contained in the U.S. Quaternary Fault and Fold (USQFF) database (http://pubs.usgs.gov/fs/2004/3033/fs-2004-3033.html). This database contains descriptions of faults known or believed to have been active during the Quaternary period (the last 1.6 million years). While particular attention should be paid to these faults in assessing the potential for induced seismicity and in siting injection operations, local faults that are suitably oriented for slip in the prevailing *in situ* stress field (see Appendix 4.B) also need to be taken into account, as does the possible presence of unmapped faults like the basement faults activated in some of the recent cases of mid-continent induced seismicity discussed above. This is further discussed in Section 4.6.3 below.

Figure 4.4-1 shows the relationship of faults to the higher-quality (quality A-C) stress measurements in central and southern California taken from the World Stress Map database (Heidbach et al., 2008), which is the most recent compilation of tectonic stress orientations, and in some cases the magnitudes of principal stress components. These measurements are derived from observations of wellbore breakouts, earthquake focal mechanisms, pressure and tiltmeter monitoring of hydraulic fractures, and geological strain indicators.

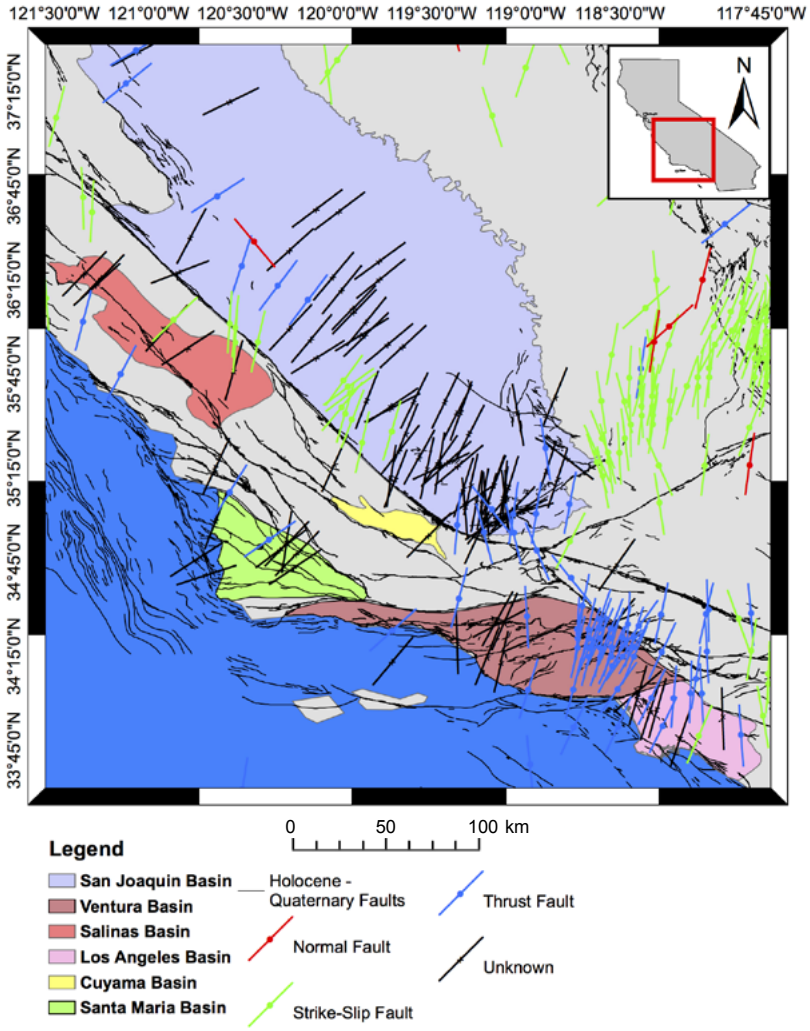

Figure 4.4-1. High-quality stress measurements for central and southern California from the World Stress Map (Heidbach et al., 2008), plotted with mapped faults from the USQFF database. The line plotted at the location of each stress measurement shows the orientation of the maximum horizontal compressive stress direction, color-coded according to stress regime.

4.4.2. California Seismicity

The generally low magnitude earthquake detection threshold in California, discussed in Appendix 4.A, means that California earthquake catalogs provide a relatively high-resolution picture of seismicity in the state as a whole. Figure 4.4-2 shows high-precision, relocated epicenters of California earthquakes M≥3 recorded in central and southern California between 1981 and 2011 contained in the Southern California Earthquake Data

Center (SCEDC) 2013 catalog (Hauksson et al., 2012). Intense seismicity occurs along segments of the major fault systems like the SAF zone in central California, in addition to relatively frequent (10s to 100s of years), large ($M_w \geq 6$) earthquakes. Large events accompanied by aftershock sequences have also occurred during this 30-year time period under the western slopes of the Central Valley near Coalinga (1983) and Kettleman Hills (1985), near Northridge (1994) and Whittier (1987, M5.9) north of Los Angeles, and along the coast near San Simeon (2003). Elsewhere, lower-magnitude seismicity is generally more diffuse. In addition to the Los Angeles Basin, oil-producing areas of the southernmost San Joaquin Valley and the Ventura Basin have relatively high rates of seismicity in the M2-5 range.

The vast majority of earthquakes in California are naturally occurring, but we can still question whether some of them may have been induced by fluid injection related to oil and gas recovery. The bulk of the seismicity that occurs in California is located at depths below about 2-3 km (1.2 – 1.9 mi). Therefore, the upper boundary of the main seismogenic zone is within about the same depth range as the deepest wastewater disposal wells for which depth information is available in the DOGGR (2014a) database, and about 1 km (0.6 mi) deeper than the depths of the wells having the highest cumulative injected volumes (see Section 4.4.3.1). Based just on the observed depths of earthquakes relative to injection depths in the reported cases of induced seismicity discussed in Section 4.3.5, it would appear that the overall potential for seismicity to be induced by wastewater injection may be at least as high in California as in the central U.S. Furthermore, some M5-6 events are observed to occur at relatively shallow depths in California, which suggests that induced earthquakes could be at least as large as those experienced to date in the continental interior. For example, ten (out of a total of 98) M5-6 earthquakes in the Hauksson et al. (2012) 1981–2011 catalog have focal depths between 3 and 6 km (1.9 and 3.7 mi), the depth range of M4 and larger induced events in the mid-continent (Section 4.3.5).

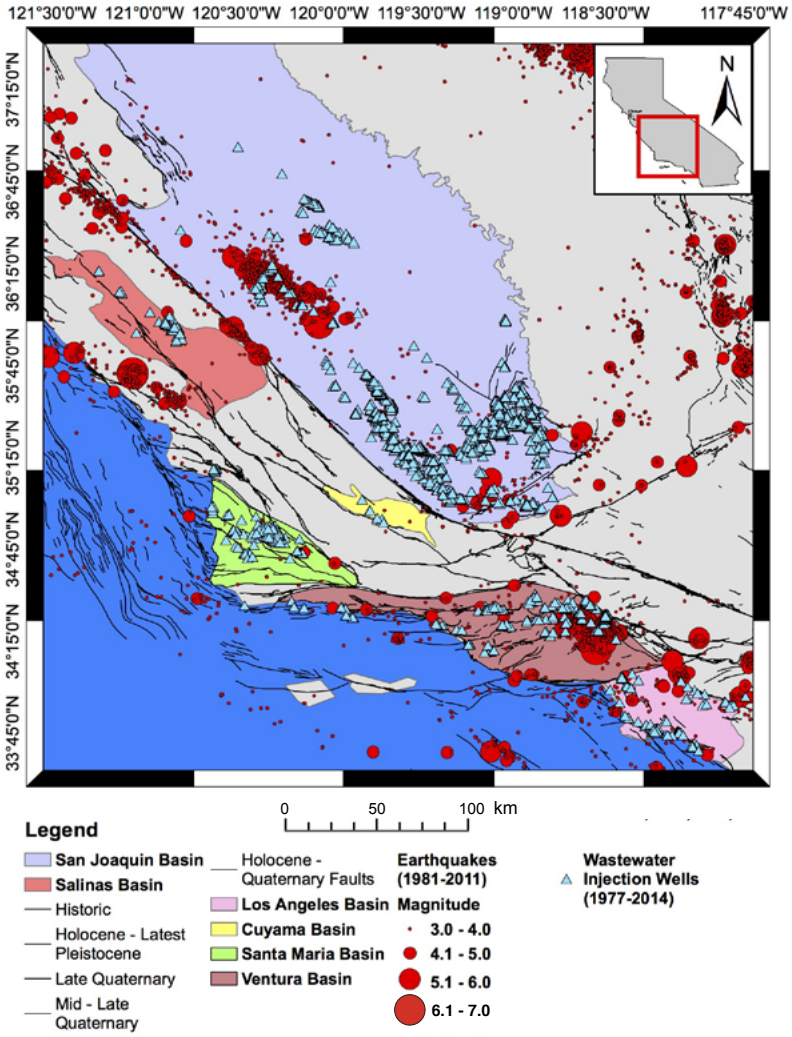

Figure 4.4-2. High-precision locations for earthquakes M≥3 in central and southern California during the period 1981-2011 (Hauksson et al., 2012), and active and previously active water disposal wells from DOGGR (2014a). Faults as in Figure 4.4-1.

While the above argument suggests that induced seismicity could potentially be caused by wastewater disposal in California, analysis of the relationship of seismicity to injection operations in the state is necessary to find out if that is indeed the case and, if so, to assess the resulting seismic hazard. Despite decades of injection in Californian oil and gas fields and one of the most active seismological monitoring and research programs in the world, no systematic study to explore possible associations between seismicity and fluid injection related to oil and gas production in the state has yet been completed. Although there have been numerous studies of induced seismicity associated with injection and production in geothermal fields in California (e.g., Eberhart-Phillips and Oppenheimer, 1984; Majer et

al., 2007; Kaven et al., 2014; Brodsky and Lajoie, 2013), and microseismic monitoring is routinely used to monitor hydraulic fracturing in oilfields (e.g., Murer et al., 2012; Cardno ENTRIX, 2012), we have found only one published paper (Kanamori and Hauksson, 1992) in which a California earthquake greater than M2 was linked to oilfield fluid injection. In that case, the authors attributed the occurrence of a very shallow M_L3.5 slow-slip event to hydraulic fracturing at the Orcutt oilfield in the Santa Maria Basin. This event was anomalous in that it radiated much lower energy at much lower dominant frequencies than normal earthquakes of similar size.

4.4.3. Correlation of Seismicity and Faulting with Injection Activity in California

One of the reasons that there have been no detailed studies of possible links between fluid injection in Californian oilfields and seismicity until recently is that small, naturally occurring earthquakes are very frequent in many regions of California, making it difficult to discriminate induced events in the M2-4 range from natural events (e.g., Brodsky and Lajoie, 2013). In contrast, natural seismicity rates are very low over most of the central and Eastern U.S., so if an earthquake does occur it is much easier to investigate whether the cause could be anthropogenic. However, Goebel et al. (2014) have reported initial results of a study that suggests that wastewater injection contributes to seismicity in Kern County, and Hauksson et al. (2014) have begun to study the relationship of seismicity to injection and production in the Los Angeles basin.

The most direct way to identify potential injection-induced seismicity on a statewide basis would be to conduct a comprehensive, systematic search for statistically significant spatial and temporal correlations between earthquake occurrence and injection rate, pressure, depth and distance from suitably oriented faults at a local scale within each oil-producing basin. A complete correlation analysis is beyond the scope of the present review. What this section does include is a summary of injection depths and volumes in California and an overview of the locations of injection wells relative to mapped faults and seismicity. Then a preliminary example of exploratory data analysis that seeks to identify relationships between injection and seismicity is presented. Given its generally higher potential for inducing seismicity of concern, we focus on wastewater disposal in California since 1981.

4.4.3.1. Depths and Volumes of California Wastewater Injection

The basic data required to carry out detailed correlation analyses include comprehensive records of the volume and pressure time histories and depths of injection in wastewater disposal wells in California. However, in the California Division of Oil, Gas and Geothermal Resources (DOGGR) database (DOGGR, 2014a), depth information is given for only 13% (329) of water disposal wells active since 1981. Reported depths range from 60 m (197 ft) to 4.42 km (14,500 ft). Of these, 21 currently active water disposal wells in their present configurations have recorded depths greater than 1.8 km (5,905 ft). The depth range for the ten highest-volume injection wells for which depth information is available is

732–838 m (2,400–2,750 ft). Compared with, for example, permitted injection intervals of 3.3–4.2 km (10,827–13,780 ft) in the Ellenberger Formation underlying the Barnett shale (Frohlich et al., 2010), the available data suggest that typical wastewater injection depths in California are about 1.5–3 km (4,921–9,842 ft) shallower than in Tarrant County in Texas, where the 2008–2009 Dallas-Fort Worth induced seismicity sequence occurred (see Appendix 4.C). However, this comparison is based on the very limited sample of California disposal wells for which depths are available.

Previous case studies show that the occurrence of induced earthquakes is usually closely associated with short-term changes in injection volume and pressure. Therefore, volume and pressure time histories sampled at intervals minutes to hours are ideally required to carry out detailed correlation analyses. However, volumes and pressures are reported on a monthly basis in the DOGGR database. The reported volume rates and pressures are assumed to be monthly averages.

Currently, average annual wastewater disposal volumes per well in California are generally less than in other regions in the U.S. where well stimulation is taking place. According to DOGGR (2010) (the most recent annual report available), total annual wastewater injected in 2009 in Kern County was approximately 79.4 million m^3 (21 billion gal) into 611 active wells, or an average disposal rate of about 360 m^3 (95,100 gal) per well per day. This, for example, is less than one-fourth of typical water disposal rates of 1,590 m^3 (420,000 gal) per well per day in Tarrant and Johnson Counties, Texas (Frohlich et al., 2010). In the Raton Basin of Colorado and New Mexico, an increase in the average daily rate of fluid injection to 300 m^3 /day (79,250 gal/day) per well, comparable to California's average daily disposal rate, was linked to a significant increase in the number of earthquakes greater than M3 (Rubenstein et al., 2014) (see Appendix 4.C), but in this case the increase in injection rate took place simultaneously in 21 wells within the basin.

In terms of cumulative volume, there are 27 wells in California that have cumulative injected volumes since 1977 greater than 16 million m^3 (4.2 billion gal), 13 of which are located on the eastern side of the southern San Joaquin Valley near Bakersfield. Further investigation is needed to determine if these 13 high-volume wells were injecting into the same pool. If this is the case, and if the wastewater was not injected into the same interval as it was produced from, then the aggregate injected volume into the pool between 1977 and 2013 was 334 million m^3 (88.2 billion gal). This is only one-half the aggregate injected volume reported for the Raton Basin during the main period of induced seismicity there between 2006 and 2013, when the 21 injection wells each disposed of 33 million m^3 (8.7 billion gal) (Rubenstein et al., 2014). The reported aggregate volume for the Raton Basin does not include the volume injected between 1995 and 2006, when the field was under development.

4.4.3.2. Locations of Wastewater Injection Wells Relative to Mapped Faults and Seismicity

Many active faults in California are not confined to the basement or deeper sedimentary layers but extend all the way to the Earth's surface. This means that in many cases the lateral distance from a disposal well to a fault is likely as important as the depth of injection in determining whether a hydraulic connection is established that allows injection-induced pressure changes to reach the fault. Although cases like the Rocky Mountain Arsenal and Raton Basin indicate that pressure perturbations large enough to induce earthquakes can travel distances up to10 km (6.2 mi) or more along fault zones, in all but one of the cases of mid-continent induced seismicity discussed in Section 4.3.5 the injection wells were located less than 3 km (1.9 mi) laterally from the fault defined by the seismicity. The exception was Paradox Valley, Colorado, where the largest event (M_w4.0 in January, 2013) induced by 17 years of continuous high-rate injection occurred on a fault located 8 km (5 mi) away from the well (Block et al., 2014). The cumulative volume injected in the Paradox Valley well between 1996 and 2012 was about 8.5 million m^3 (2.2 billion gal), about half of typical cumulative volumes injected into the 27 highest-volume wastewater disposal wells in California since 1977. It is important to note that there is a high-permeability pathway between the Paradox Valley well and the fault activated in the 2013 event, which apparently corresponds to a regional-scale fracture zone (King et al., 2014).

These well-fault distances provide the context for the following brief summary of spatial relationships between wastewater injections wells and surface faults and seismicity in oil-producing basins in California.

Figure 4.4-3 summarizes the distribution of distances between wastewater disposal wells active since 1981 and faults in the USQFF database in six oil-producing basins in California. Across all six basins, over 1,000 wells are located within 2.5 km (1.5 mi) of a mapped active fault, and more than 150 within 200 m (656 ft).

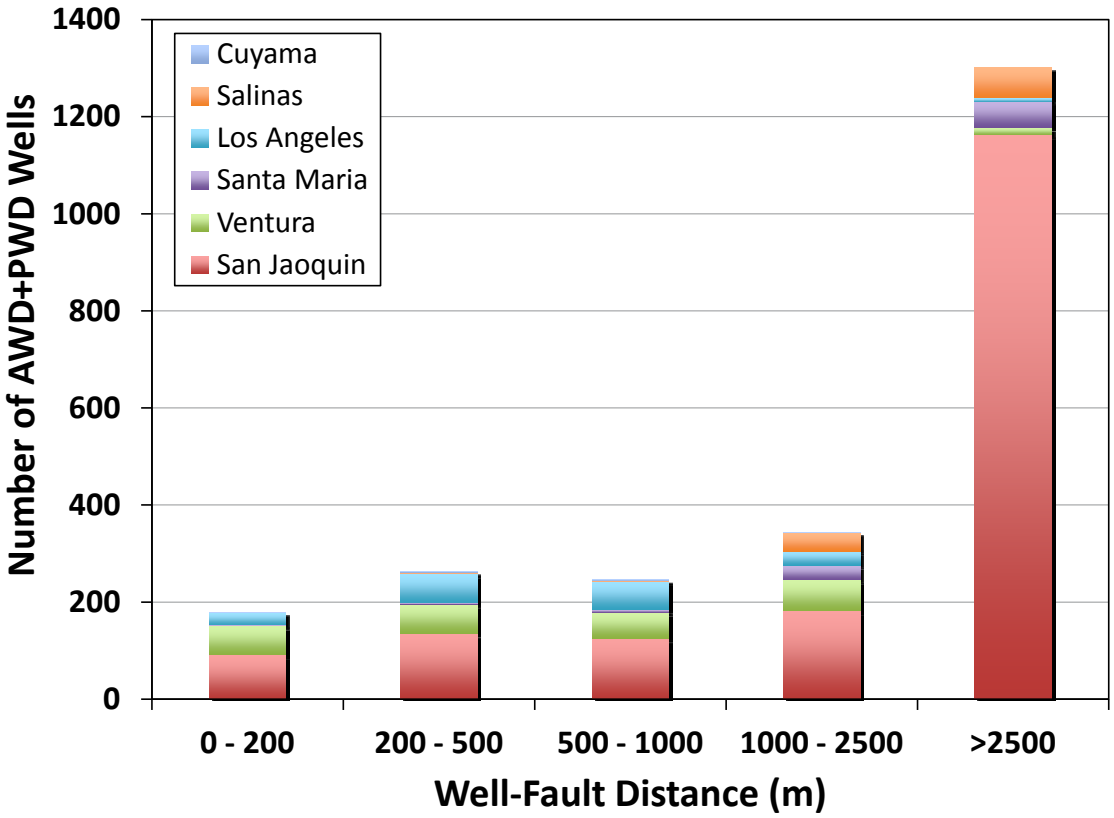

Figure 4.4-3. Distribution of distances between wastewater disposal wells active during the period 1981-present (DOGGR, 2014a) and Quaternary active faults in the six major oil-producing basins in California.

The maps in Figures 4.4-4 to 4.4-9 show the locations of disposal wells relative to mapped faults and seismicity in four of the largest oil-producing basins. The faults are colored according to the estimated time of their last earthquake activity as follows: historic (red), <~150 years; Holocene/latest Pleistocene (orange), <15,000 years; latest-Quaternary (yellow), <130,000 years; Quaternary (blue), <1.6 million years. The most recently active faults and those with the highest long-term slip rates are considered to be the ones most likely to experience future earthquakes. Long-term slip rates of California faults range from less than 0.1 mm/yr to 34 mm/yr on the SAF.

The historically active trace of the White Wolf fault (slip rate 2 mm/yr) delineates the southeastern boundary of the San Joaquin Valley (Figures 4.4-4 and 4.4-5). This fault last ruptured in the 1952 M7.3 Kern County earthquake. (Other red traces on Figures 4.4-5 and 4.4-6 are ground fractures mapped following the 1952 earthquake or have been linked to oilfield subsidence, and so they might not correspond to active faults.) The closest well to the White Wolf fault is about 5 km (3.1 mi) south the surface trace (Figure 4.4-5). The densest concentration of seismicity is located to the southwest, where two

Quaternary faults continue the trend of the historic White Wolf trace, and Holocene and Quaternary traces of the Pleito fault system are also mapped. In addition to abundant microseismicity, M4.7 and M5.1 earthquakes occurred in this area in 2005. Several injection wells are located within 1 km (0.6 mi) of a Quaternary strand of the Pleito system. Clusters of microearthquakes have occurred close to several of the injection wells in this area, but others are located away from the wells.

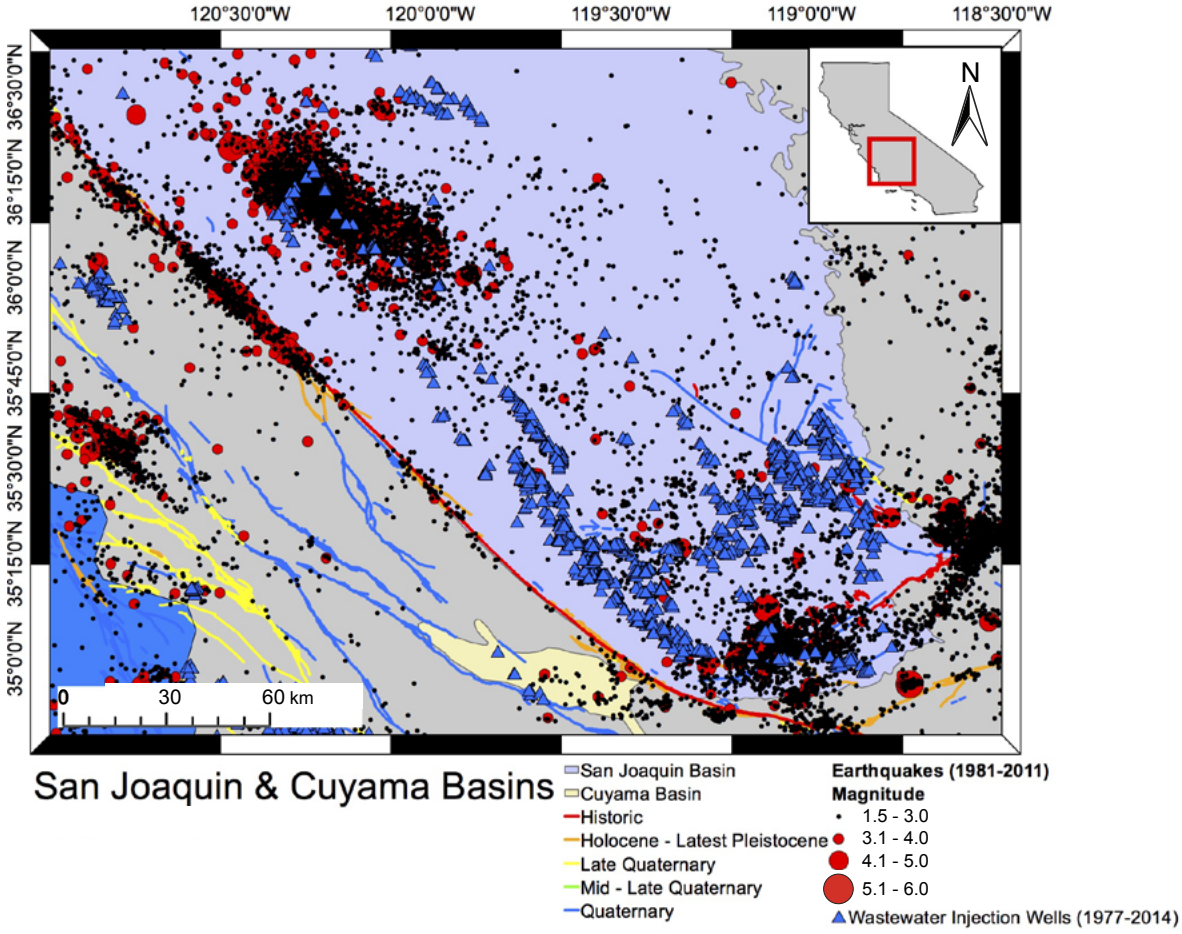

Figure 4.4-4. Earthquakes M≥1.5 in the southern San Joaquin Valley and Cuyama Basin from Hauksson et al. 2012, plotted with active and previously active water disposal wells from DOGGR (2014a) and faults from the USQFF database. Faults colored according to the time of most recent activity. The White Wolf fault is the red trace in the southeast corner of the Valley.

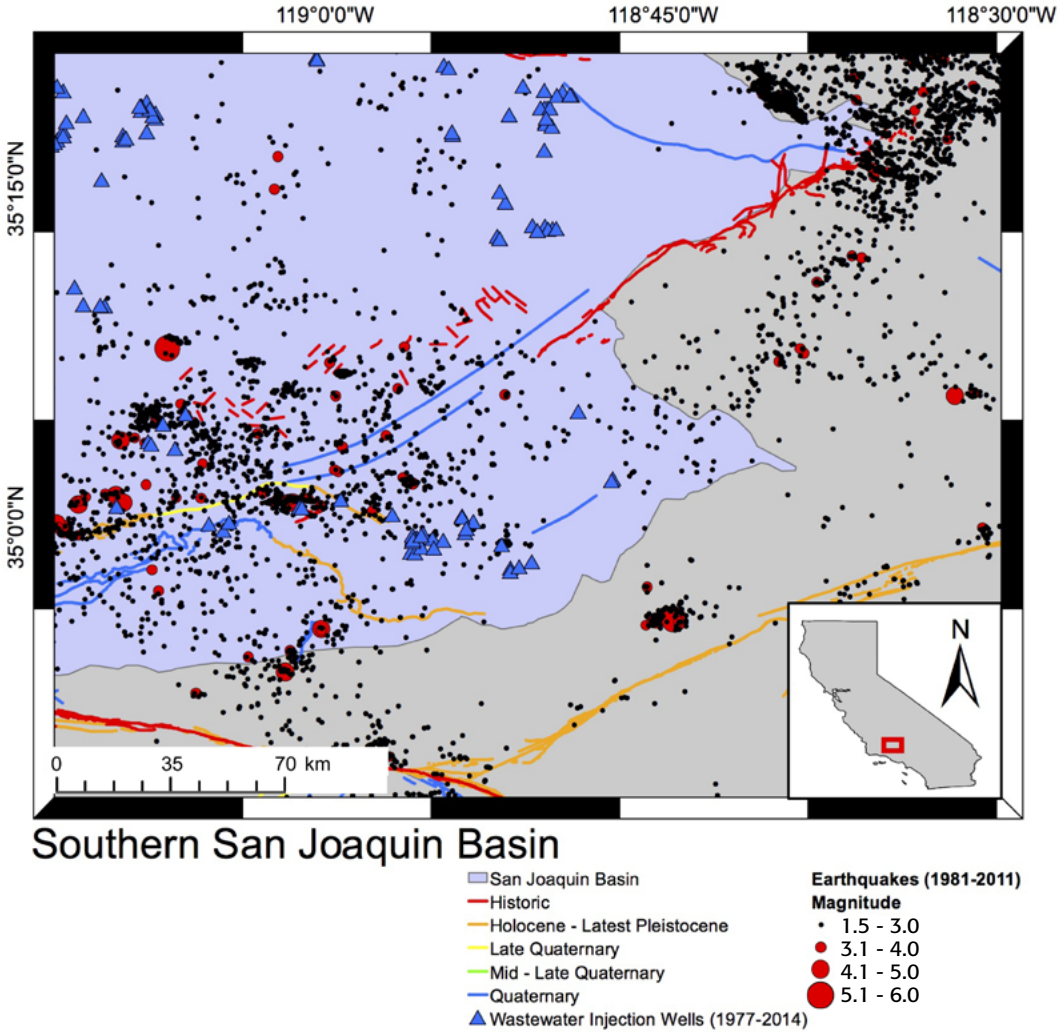

Figure 4.4-5. Earthquakes M≥1.5 in the southernmost San Joaquin Valley from Hauksson et al. (2012). Wells and faults as in Figure 4.4-4.

Quaternary and latest-Quaternary faults are mapped at the surface near the dense concentrations of disposal wells towards the eastern margin of the San Joaquin Valley in the vicinity of Bakersfield (Figure 4.4-6). Many of the Quaternary faults strike roughly north-south and are not favorably oriented for reactivation within the prevailing stress field (Figure 4.4-1). The green triangles show the locations of 13 of the 27 disposal wells in California having cumulative injected volumes greater than 16 million m^3 (4.2 billion gal). Earthquakes are observed only infrequently in this area. There is also only sparse, scattered seismicity near the long chain of disposal wells along the southwestern margin of the San Joaquin Valley (Figure 4.4-4). Most of the earthquakes in the dense cluster further northwest are aftershocks of M_w6.5 and M_w6.1 earthquakes that occurred in 1983 and 1985, respectively on deeply buried (blind) faults (U.S. Geological Survey, 1990; Ekström et al., 1992).

In the Santa Maria Basin, numerous wastewater disposal wells are located within 1–2 km (0.6–1.2 mi) of the surface traces of favorably oriented northwest-striking latest-Quaternary and Quaternary fault systems (Figure 4.4-7). All of the faults close to oilfields in the Santa Maria Basin have estimated slip rates less than 1 mm/yr (see California Geological Survey, 1996). The only dense cluster of seismicity is in the vicinity of the group of wells in the east-central part of the basin located in the Zaca oilfield. This cluster is discussed in Section 4.4.3.3 below. Numerous disposal wells in the Ventura Basin are sited very close to mapped Holocene-active faults, most notably along the major, west-striking Holocene San Cayetano system (slip rate 6 mm/yr) in the northern part of the basin, and to latest-Quaternary faults (Figure 4.4-8). Pockets of dense seismicity are located both close to and remote from injection wells. Most of the events in the dense cloud of seismicity at the eastern end of the basin are aftershocks of the deep (21 km; 13 mi) 1994 Northridge earthquake.

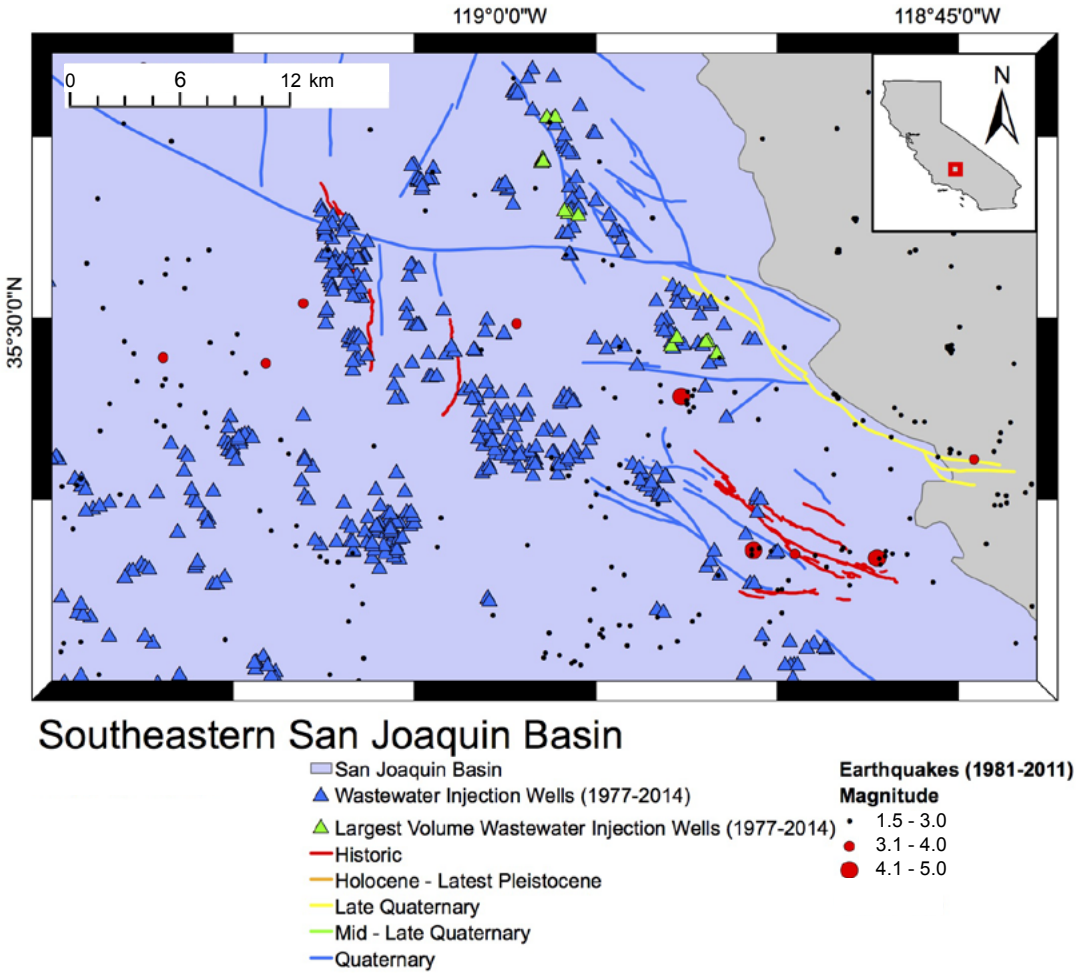

Figure 4.4-6. Earthquakes M≥1.5 in the southeastern San Joaquin Valley near Bakersfield from Hauksson et al. (2012). Wells having cumulative injected wastewater volumes >16 million m³ (4.2 billion gal) shown in green. Other wells and faults as in Figure 4.4-4.

In the Los Angeles Basin (Figure 4.4-9), disposal wells are concentrated mainly in oilfields located along the Holocene Newport-Inglewood fault zone (slip rate 1.5 mm/yr), a segment of which was the source of the destructive 1933 M_w6.4 Long Beach earthquake, and in the Wilmington oilfield. Several wells in the Wilmington field are located within 4 km (2.5 mi) of the Holocene Palos Verdes fault (slip rate 3 mm/yr). Only scattered seismicity has occurred near any these fields except Inglewood and Cheviot Hills at the northwestern end of the Newport-Inglewood trend. As in the Ventura Basin, clusters of seismicity are located close to some disposal wells but also elsewhere. The cluster at the top-center of the figure are aftershocks of the 2014 La Habra earthquake.

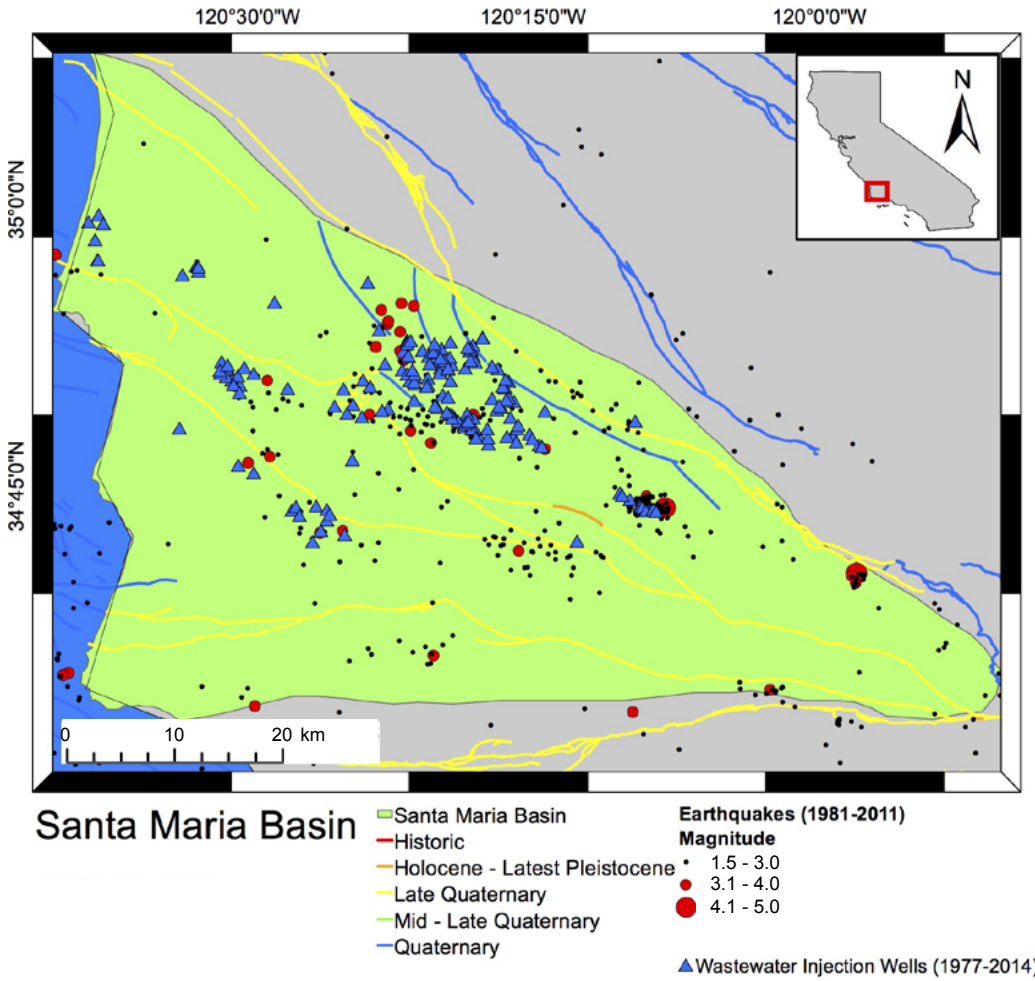

Figure 4.4-7. Earthquakes M≥1.5 in the Santa Maria Basin from Hauksson et al. (2012). Wells and faults as in Figure 4.4-4.

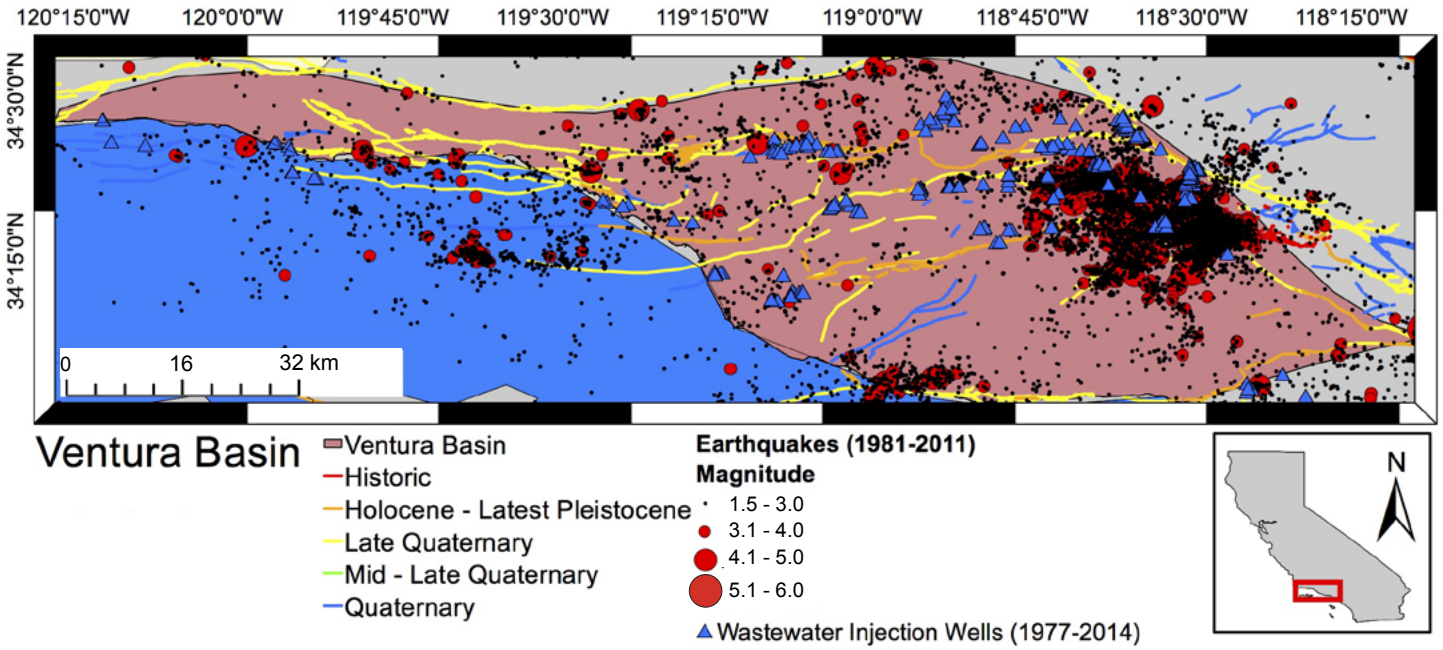

Figure 4.4-8. Earthquakes M≥1.5 in the Ventura Basin from Hauksson et al. (2012). Wells and faults as in Figure 4.4-4.

While numerous disposal wells in some of the basins are located very close to active faults, not all of those necessarily have the potential for inducing seismicity. In some cases injection may be into a depleted zone, in which years of oil production has reduced the pressure below its pre-drilling state, thus increasing the resistance to slip on faults in hydraulic connection with the reservoir (NRC, 2013). (Note that disposal into depleted reservoirs is distinct from reinjection of wastewater for enhanced oil recovery by water flooding; waterflood wells are listed separately in the DOGGR database.) In these cases, the potential for induced seismicity will not exist until the pressure buildup resulting from injection exceeds the original reservoir pressure. The DOGGR Online Well Record Search (DOGGR, 2014b) tool details the pool(s) into which each disposal well injects, so it should be possible to determine which wells inject into depleted zones by examining the production records for the same pool.

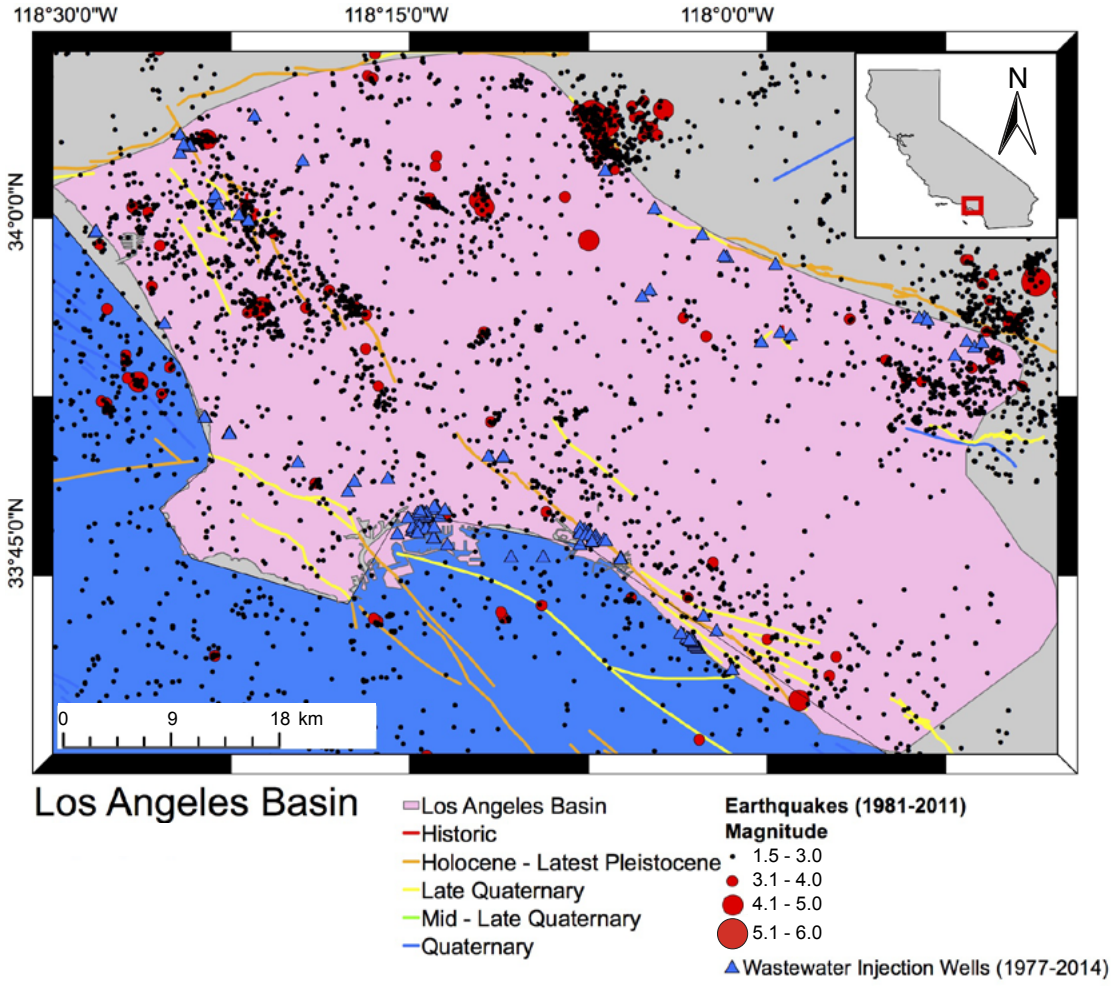

Figure 4.4-9. Earthquakes M≥1.5 in the Los Angeles Basin from Hauksson et al. (2012). Wells and faults as in Figure 4.4-4.

4.4.3.3. Preliminary Example of a Spatiotemporal Correlation Analysis

To analyze potential correlations of seismicity with water injection, we first identify clusters of earthquakes and then examine the relationships of the clusters to injection volumes and pressures. This is illustrated for the Santa Maria Basin in Figure 4.4-10. Figure 4.4-10a shows 1981–2011 Santa Maria Basin earthquake epicenters in the Hauksson (2012) catalog. To easily identify event clusters, each epicenter is color coded according to the slant distance (i.e., including event depth) of the event hypocenter to its nearest neighbor. Figure 4.4-10b shows the highly clustered seismicity contained in the green rectangle in 4.4.10a at expanded scale and the spatial relationship of the events to the locations of injection wells in the Zaca oilfield. Figures 4.4-10c and 4.4-10d compare the occurrence history of these 66 earthquakes with injected fluid volume and pressure histories for the four injection wells shown colored in Figure 4.4-10b. All of the events

occurred between October 1984 and March 1987, and all but a few are clustered in two bursts of activity in October 1984 and October-November 1986. Both bursts include one event greater than M4.

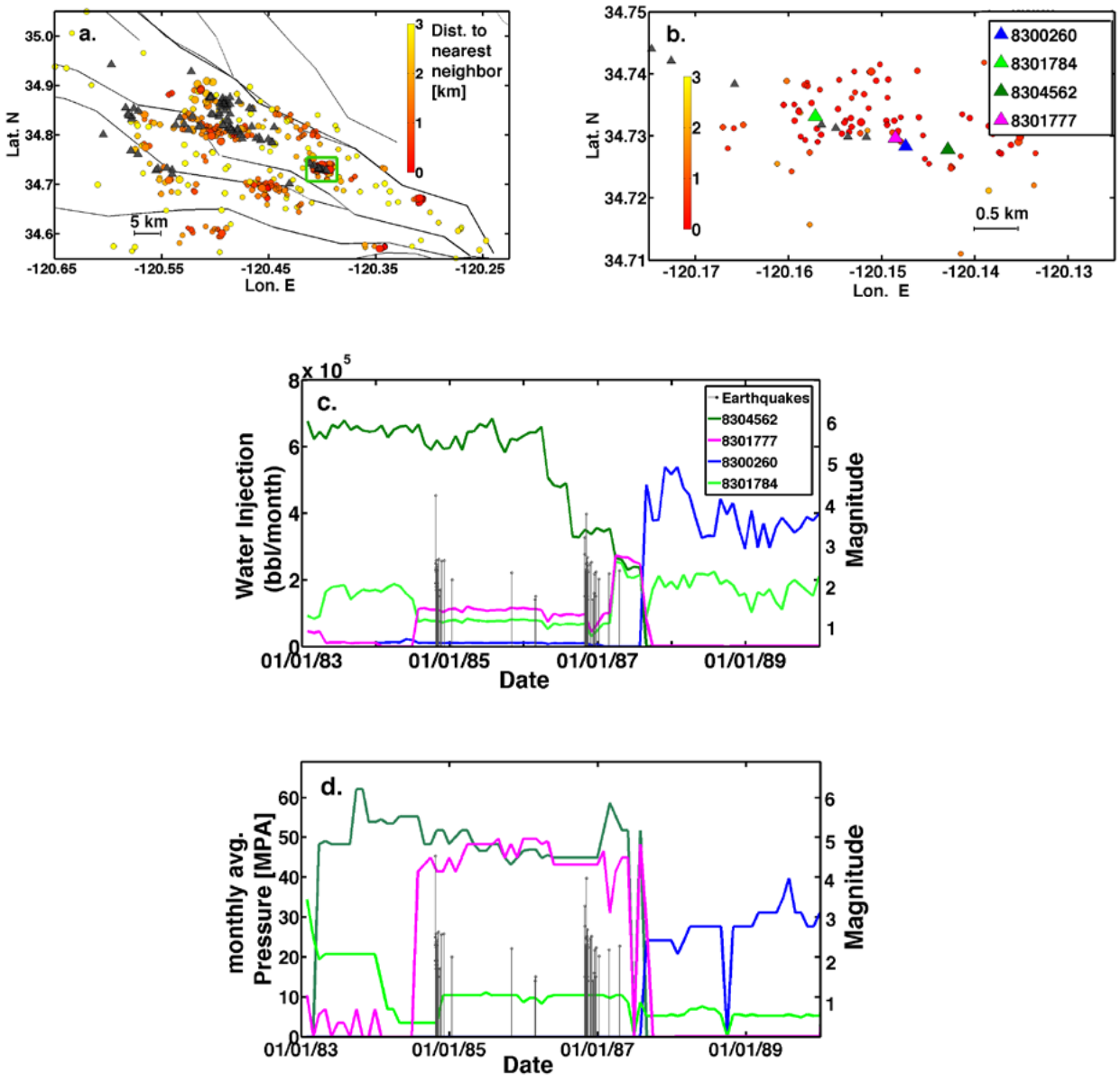

Figure 4.4-10. Spatiotemporal analysis of a seismicity cluster in the Santa Maria Basin. Earthquakes shown by solid circles in a and b are color-coded to show their closest slant distances to neighboring events. Wastewater injection wells are shown as triangles. Events and wells within the green rectangle in a are shown in b. Monthly injected volumes and wellhead pressure taken from the DOGGR (2014a) database for the four wells colored in b and identified by API number are plotted in c and d, respectively, along with the earthquakes in b shown in black.

The first burst of seismicity occurred about one month after the pressure in well 8301777 (magenta) reached its first peak following the abrupt increase in injection rate and pressure that began in June 1984, and also coincides with the beginning of a modest increase in pressure in well 8301784 (light green). These correlations suggest a relationship between the event sequence and the combined effect of the pressure increases in these two wells, which are the wells closest to the most densely clustered seismicity in Figure 4.4-10b. The second burst of activity was not associated with pressure changes apparent in the DOGGR database, but occurred shortly after a major decrease in injection rate in well 8304562 (dark green). In this case, no immediate correlation with changes in pressure in any of the wells is evident. However, all 66 earthquakes occurred during a period when the pressures in wells 8301777 and 8301784 (and also in well 8304562) were high, which further suggests a relationship between local seismicity and elevated fluid pressure. These evident relationships merit further detailed analysis that includes tests of statistical significance to investigate whether there is a causal link between the seismicity and pressure changes. Note that the flat portions of the pressure histories for the three wells mentioned above between May and December 1986 suggest missing data for this period, so that the pressure increase in well 8304562 (and in 8300260) evident after December 1986 may have begun earlier, perhaps following a pressure decrease sometime after May 1986.

This simple example demonstrates that analysis of the spatial and temporal relationship of earthquakes to wastewater injection has the potential to detect and characterize induced seismicity in California. However, the apparent gaps in the pressure data for several periods evident in Figure 4.4-10d, and the lack of depth information for any of the disposal wells in the Zaca field, illustrate two of the deficiencies in the present DOGGR well database that impede this kind of correlation analysis (see Section 4.6.1 below).

4.4.4. Potential for Induced Seismicity on the San Andreas Fault

The existing oilfields and disposal wells closest to the SAF are located just over 10 km (6.2 mi) away along the western margin of in the San Joaquin Valley (Figure 4.4-4). This is significantly greater than typical lateral well-fault distances of less than 3 km (1.9 mi) for the fluid injection-induced seismicity cases observed in the continental interior (see Section 4.4.3.2). It is similar to the 8 km (5 mi) distance between the Paradox Valley injection well and the fault that was the source of the 2013 M_w4.0 earthquake, but in that case a high-permeability pathway connects the well to the fault (Section 4.4.3.2). Therefore, while the possibility that current, relatively low-volume, wastewater injection in the San Joaquin Valley could induce earthquakes on the SAF cannot be entirely discounted, we judge that that it is unlikely.

Using the Paradox Valley case as a benchmark, it is plausible that the likelihood of triggering earthquakes on the SAF could increase if future high-volume wastewater injection took place in or close to existing disposal wells along the western margin of

the San Joaquin Valley. Future injection projects that could potentially alter fluid pressures in the SAF or the other most active (high slip rate), major fault zones should be subject to particularly rigorous screening and permitting procedures, as described in the following section.

4.5. Impact Mitigation

Even if a comprehensive investigation of the relationship of seismicity to oilfield injection were to conclude that the overall potential for induced seismicity in California is low, it would be prudent to adopt measures to mitigate the risks from induced seismicity that may be associated with new stimulation-related injection projects. It will be particularly important to adopt such measures if there is an increase in stimulation activity and expanded production, resulting in higher per-well volumes of injected wastewater approaching those employed elsewhere in the U.S. In this section, we discuss measures that should be considered before injection begins to reduce the likelihood of induced earthquakes, and to manage seismicity during and following injection.

Initial, low-level hazard and risk assessment during site screening could be used to place each site into one of a few risk categories (e.g., low, moderate, high), based on the following recommended criteria:

- Planned injection rate, cumulative volume, duration, and depth.
- Distance from active or potentially active faults, and recency and rate of fault activity.
- Existence of potential high-permeability pathways between the well and faults
- Estimation of pressure changes on nearby faults.
- Background seismicity.
- Proximity to population centers and critical facilities.

Decisions regarding permitting and regulation of a site in one of the higher risk categories could then be based on a level of probabilistic seismic hazard and risk assessment determined to be appropriate for that category. The final permit would specify operating parameters such as maximum injection rate and pressure adjusted to achieve an acceptable level of risk. An important part of the permit would be specifications for monitoring requirements and operating procedures to manage and, if necessary, mitigate induced seismicity during injection, and perhaps for a period after the well is shut down. Methods for induced seismicity hazard and risk assessment and management are discussed in Section 4.5.1 below.

If future large-volume wastewater disposal were to be planned at sites along the western margin of the San Joaquin Valley, and especially if new injection locations closer to the SAF and other major active faults were contemplated, these wells should be subject to the most stringent risk assessment and permitting requirements. These should include detailed modeling to estimate the probability that the pressure changes on the fault over time would remain below a predetermined, conservative maximum bound.

4.5.1. Induced Seismic Hazard and Risk Assessment

Maps of seismic hazard from naturally occurring earthquakes in California are developed by the U.S. Geological Survey (USGS) and California Geological survey (CGS) as part of the National Seismic Hazard Mapping Project. The hazard maps and technical details of how they are produced can be found at http://earthquake.usgs.gov/hazards/index.php. Of the areas in which water disposal wells are currently active, seismic hazard from naturally occurring earthquakes is high in the Los Angeles, Ventura, Santa Maria, Salinas and Cuyama Basins and in the Santa Clarita Valley, and moderate to high along the western and southern flanks of the southern San Joaquin Valley. The hazard is moderate in the Bakersfield area and decreases towards the center and north of the San Joaquin Valley.[1]

Approaches to assessing induced seismicity hazard can be developed by adapting standard probabilistic seismic hazard assessment (PSHA) methods, such as those used by the USGS and CGS. The standard methods cannot be applied directly, however, because conventional PSHA usually is based only on mean long-term (100s to 1,000s of years) earthquake occurrence rates; i.e., earthquake occurrence is assumed to be time-independent. Induced seismicity, on the other hand, is strongly time- and space-dependent because it is dependent on the evolution of the pore pressure field, which must therefore be considered in estimating earthquake frequencies and spatial distributions.

Developing a rigorous PSHA method for short- and long-term hazards from induced seismicity presents a significant challenge. In particular, no satisfactory method of calculating the hazard at the planning and regulatory phases of a project is available at the present time; whereas in conventional PSHA earthquake frequency-magnitude statistics for a given region are derived from the record of past earthquakes, obviously no record of induced seismicity can exist prior to well stimulation or wastewater disposal. Using seismicity observed at an assumed “analog” site as a proxy (e.g., Cladouhos et al., 2012) would not appear to be a satisfactory approach, as induced seismicity is in general highly dependent on site-specific subsurface structure and rock properties.

1. Moderate and high seismic hazard are defined here as a 2% probability of exceeding peak ground accelerations of 0.1-0.3g and greater than 0.3g, respectively, in 50 years, where g is the acceleration due to gravity. The threshold of damaging ground motion is about 0.1g.

Physics-based approaches to generate simulated catalogs of induced seismicity at a given site for prescribed sets of injection parameters are under development (e.g., Foxall et al., 2013). Such approaches rely on adequate characterization of the site geology, hydrogeology, stress, and material properties, which are inevitably subject to significant uncertainties. However, large uncertainties in input parameters are inherent in PSHA in general, and techniques for propagating them to provide rigorous estimates of the uncertainty in the final hazard have been developed (e.g. Budnitz et al., 1997).

There has been more progress in developing methods for short-term hazard forecasting based on automated, near-real time empirical analysis of microseismicity recorded by a locally deployed seismic network once injection is under way (e.g., Bachmann et al., 2011; Mena et al., 2013; Shapiro et al., 2007). Continuously updated hazard assessments can form the input to a real-time mitigation procedure (Bachmann et al., 2011; Mena et al., 2013), as outlined in Section 4.5.2. Using two different time-dependent empirical models, Bachmann et al. (2011) and Mena et al. (2013) retrospectively were able to obtain acceptable overall fits of forecast to observed seismicity rates induced by the 2006 Enhanced Geothermal System (EGS) injection in Basel, Switzerland, over time periods ranging from 6 hours to 2 weeks. However, the models performed relatively poorly in forecasting the occurrence of the largest event (M_L3.4), which occurred after well shut-in; this event was forecast with a probability of only 15%, and the forecast probability of exceeding the ground motion it produced was calculated at only 5%. The performance of this empirical method could probably be improved by incorporating a more physically based dependence on injection rate or pressure.

4.5.2. Protocols and Best Practices to Reduce the Impact of Induced Seismicity

In 2004, the U.S. Department of Energy (DOE) and the International Energy Agency (IEA) sponsored an effort to develop a protocol and best practices to monitor, analyze, and manage induced seismicity at geothermal projects (Majer et al., 2007; 2012; 2014). The protocols/best practices are not intended to be either regulatory documents or universally prescribed sets of procedures for induced seismicity management, but rather to serve as a guide to enable stakeholders to tailor operating procedures to specific projects. Many geothermal operators in the western U.S. are implementing either all or parts of the most recent U.S. DOE protocol (Majer et al., 2012), and the U.S. Bureau of Land Management (BLM) has adopted it as the basis for developing criteria for geothermal project permitting on the federal lands administered by them.

Largely spurred by the dramatic increase in seismicity in the mid-continent discussed in Appendix 4.C, oil-producing states and the petroleum industry are beginning to develop similar protocols, such as those being developed by the Oklahoma Geological Survey and by a consortium of member companies in the American Exploration and Production Council (AXPC) (see Appendix 4.D). Zoback (2012) also describes a series of mitigation steps that operators could use as a guide. All of the protocols currently under development contain, in some combination, the steps that comprise the U.S. DOE geothermal protocol, described in Appendix 4.D.

Current real-time induced seismicity monitoring and mitigation strategies used by most enhanced geothermal system (EGS) operators employ a "traffic-light" system similar to the one implemented by Bommer et al. (2006). The traffic-light system may incorporate up to four stages of near-real time response to recorded seismicity, ranging from normal operation (green) to bleeding off to minimum wellhead pressure and shutting down the well (red). The response trigger criteria are generally based on some combination of maximum observed magnitude, measured peak ground velocity and public response, although definition of the criteria is usually somewhat ad hoc and depends on the project scenario. The traffic-light procedure implemented at the 2006 Basel EGS project was not successful in preventing the occurrence of the M_L3.4 earthquake that led to the eventual abandonment of the project, even though the well was shut down following an earlier M_L2.7 event. The EGS community is beginning development of traffic-light methods that employ near-real time hazard updating like that reported by Bachmann et al. (2011) and Mena et al. (2013). These will provide risk-based forecasting based on the evolving seismicity and state of the reservoir to inform decision-making.

4.6. Data Gaps

4.6.1. Injection Data

There are two important gaps in the current DOGGR (2014a) injection database that seriously limit its usefulness for investigating induced seismicity in California. First, injection rates and wellhead pressures are reported monthly. These are presumably monthly averages, since water disposal rates and pressures are rarely constant over month-long intervals. Significant short-term variations in peak pressures and injection rates are relevant to detecting the effects of fluid injection on seismicity in the vicinity of the well, in addition to long-term rates and cumulative volumes that can potentially impact seismicity on more distant faults. Therefore, monthly averages are usually too coarse to carry out correlation analyses against incremental increases in seismicity above the high seismic background in many areas of California.

The second data gap is consistent and accurate reporting of injection depth and geological interval. Currently, depth information of any kind is provided for less than 15% of active and plugged wastewater disposal wells in the database. Furthermore, currently available information is ambiguous because the parameter "WellDepthAmount" in the database can refer to injection depth, top or bottom of the perforation interval, or the total vertical depth of the well. Correlating injection depth with stratigraphy and the depth of seismicity has been shown to be critical in identifying induced events (e.g., Keranen et al., 2013).

Although it may be feasible to conduct spatiotemporal correlation analyses to identify and provide a basic characterization of more prominent cases of potentially induced seismicity using the current DOGGR (2014a) database, filling these two data gaps to some extent in the existing catalog would permit a much more comprehensive analysis. More complete reporting in the future would enable risk assessment and mitigation of induced seismicity for new stimulation-related injection operations.

4.6.2. Seismic Catalog Completeness

Although only earthquakes greater than about M2 are generally relevant to seismic hazard, M1 or even smaller earthquakes are important in analyzing potential induced seismicity. As discussed in Appendix 4.A, the estimated minimum magnitude of complete detection (M_c) of the USGS Advanced National Seismic System (ANSS) network is M1 or less in large areas of California, and less than M2 over most of the state. However, Figure 4A-1 shows that M_c is between 2 and 2.5 in the interior of the southern San Joaquin Valley and at some locations along the coast of southern California. Estimated mean, minimum and maximum M_c values in the main onshore oil-producing basins are summarized in Table 4.6-1; note that these values have not been adjusted to account for the tendency of the calculation method employed to underestimate M_c (see Appendix 4.A). Some wells in the southern San Joaquin Valley and the Los Angles and Ventura Basins are within areas having M_c2 or greater, so that microseismicity that may have been induced by injection into those wells might not have been recorded.

Ideally, a sensitive local seismic network comprising five or more seismic recording stations deployed at a spacing on the order of one kilometer or less is required to provide an adequate characterization of both the background activity and any induced seismicity at an injection site. Deploying sensors in deep boreholes is relatively expensive, but greatly enhances the signal-to-noise ratio, enabling very small earthquakes (often $M < 0$) to be recorded. While installation of a local network may not be feasible or necessary at many injection sites, it should be considered for sites in higher risk categories (Section 4.5).

4.6.3. Fault Detection

The USQFF fault inventory described in Section 4.4.1.2 contains the parameters of Quaternary-active faults in California. While it will be important to consider these faults in siting possible new injection operations, smaller local faults in the site vicinity will likely be of more direct relevance in assessing the potential for induced seismicity. These include faults having lengths on the order of 1 to 10 km (0.6–6.2 mi) capable of producing earthquakes between about M_w3.5 and 5, and even smaller ones that are potential sources of felt earthquakes. The fault inventory should also include inactive faults (i.e., activity predates the Quaternary) that are suitably oriented relative to the *in situ* stress field for shear failure. Both major and local faults that outcrop at the surface are shown on published geologic maps at scales as large as 1:24,000 (USGS 7.5 minute quadrangles). Unmapped faults on the kilometer scale, including buried structures, may be detectable in seismic and well data acquired during field exploration or characterization of specific injection sites. Faults on the 100-meter scale may be detectable depending on specific circumstances, but in general present a greater challenge. Finally, faults that are potential sources of induced earthquakes of concern and that escape detection during site characterization may often be illuminated by low-magnitude microearthquakes recorded during the initial stages of injection.

Table 4.6-1. Summary of minimum magnitudes of complete detection, M_c, in onshore oil-producing basins. M_c values not adjusted to accountt for underestimation bias (see Appendix 4.A).

Basin	Mean M_c±1s	Min M_c	Max M_c
Los Angeles	1.5±0.2	1.1	2.0
Ventura	1.5±0.3	0.8	2.1
Santa Maria	1.6±0.3	1.1	2.1
Cuyama	1.4±0.2	0.9	1.7
San Joaquin	1.6±0.3	0.6	2.0
Salinas	1.0±0.3	0.3	1.3

4.6.4. In-situ Stresses and Fluid Pressures

Although there are a large number of stress measurements in California compared with other regions of the U.S., the point measurements in the World Stress Map database provide only a sparse sampling of the stress field. While overall trends in Figure 4.4-1 appear relatively uniform, significant variations are to be expected because stress states at the local scale are influenced by heterogeneously distributed fractures of varying orientation and by changes in lithology and rock material properties (e.g., Finkbeiner et al., 1997). Ideally, stress measurements at a given injection site are needed to assess the potential for induced seismicity. To achieve this, it may be possible to employ other measurement techniques in addition to borehole data and analysis of hydraulic fracture breakdown and shut-in pressures. For example, in a hydraulic fracturing experiment in the Monterey formation, Shemeta et al. (1994) studied the geometry of the hydrofracture using continuously recorded microseismic data, regional stress information, and well logs. They found that the microseismic and well data were consistent with both the regional tectonic stress field and fracture orientations observed in core samples and microscanner and televiewer logs. The results of this study suggest that observations of the natural fracture system can be used as indicators for the orientations of induced fractures and hence of the *in situ* stress. As with local microseismic monitoring, *in situ* stress measurements may be justified only at higher-risk sites. However, measurement or estimation of stress orientations prior to well stimulation is critical for selecting a development well pattern and the design of hydraulic fractures for effective hydrocarbon recovery. Such measurements can be used to inform induced seismic hazard assessment for well stimulation activities within a field, and also for any nearby wastewater disposal operations.

4.7. Findings

The dramatic increase in the rate of earthquake occurrence that has accompanied the boom in unconventional oil and gas recovery in the central and eastern U.S. since 2009 has highlighted the fact that injecting fluids into the subsurface for well stimulation by hydraulic fracturing—and, in particular, for disposal of recovered fluids and produced wastewater—can cause induced seismicity. Induced seismicity can occur when fluid

injection results in increased pore pressure within a fault. This reduces the force holding the two sides of the fault together, allowing the fault to slip.

Hydraulic fracture treatments inject relatively small volumes injected over short time periods. As a result, the subsurface volume affected by pressure perturbations is normally within hundreds of meters from the injection well, which, current experience suggests, limits the size of induced seismic events caused by well stimulation. To date, the largest event generally considered to have been caused by hydraulic fracturing is the 2011 M_L3.8 earthquake in the Horn River Basin in British Columbia (BC Oil and Gas Commission, 2012).

Injection of large volumes of wastewater over long time periods increases pressures over much larger distances than those resulting from hydraulic fracturing, which increases the likelihood of inducing larger seismic events. Therefore, injection of wastewater presents a much larger potential seismic hazard than hydraulic fracturing. The largest earthquake suspected of being related to wastewater disposal is the 2011 M_w5.7 Prague, Oklahoma event (Keranen et al., 2013; Sumy et al., 2014), but the causal mechanism of this event is still the subject of active research. The possibility that this was a naturally occurring tectonic earthquake cannot yet be confidently ruled out. The largest earthquake for which there is clear evidence for a causative link to stimulation-related wastewater injection is the 2011 M_w5.3 event in the Raton Basin, Colorado (Rubinstein et al., 2014).

The potential impacts from ground shaking caused by induced seismicity are structural damage—and possibly injuries and loss of life—and nuisance resulting from seismic events that are felt in nearby communities. While the vast majority of fluid injection-induced earthquakes are too small to be perceptible at the ground surface, some are strongly felt and on rare occasions can be large enough to cause damage (e.g., Kerenan et al., 2013; Rubinstein et al., 2014). The magnitude threshold for local structural damage is generally considered to be about M_w5, depending on the depth of the earthquake, surface site conditions, and the fragility of nearby structures. To date, the maximum magnitudes of earthquakes induced by hydraulic fracturing worldwide have been substantially below this threshold, which suggests that the likelihood of seismic damage resulting from hydraulic fracturing in general is very low.

The likelihood of damaging events resulting from wastewater disposal is much higher than that from hydraulic fracturing. Four earthquakes greater than M4.5 related to wastewater disposal have occurred in the U.S. since 2011 (see Appendix 4.C), of which the 2011 Prague and Raton Basin events mentioned above caused localized structural damage. However, given that induced seismicity has been associated with only a small fraction of the tens of thousands of injection wells currently or formerly active in the U.S., viewed in a global context the overall likelihood of a damaging event being induced by wastewater injection is low in absolute terms.

The magnitude threshold for felt events can be as low as M1.5–2.0 for the shallow depths of seismicity that are typically associated with fluid injection. There are only five documented cases of seismicity related to hydraulic fracturing worldwide that included

felt events, but numerous cases related to wastewater injection. Because, in general, the rate of earthquake occurrence increases by about a factor of ten for every decrease of one magnitude unit, the overall likelihood of nuisance from wastewater injection-induced earthquakes is relatively high.

4.8. Conclusions

Although induced seismicity occurs at several geothermal fields in California, there have been no published reports of felt seismicity linked to either hydraulic fracturing or wastewater disposal in the state, apart from one highly anomalous event reported by Kanamori and Hauksson (1992). However, in many areas of California, discriminating induced events in the M2-4 range from frequently occurring natural events is difficult, and the systematic studies necessary have begun only recently.

The lack of reported felt seismicity related to hydraulic fracturing is consistent with injection into predominantly vertical wells at relatively shallow depths in California and the small injection volumes currently employed. Therefore, based on experience elsewhere, hydraulic fracturing as currently carried out in California is not considered to pose a high seismic risk.

The total volume of wastewater injected in California is much larger than the volume used for well stimulation, but current volumes are relatively small compared to the regions in the U.S. that have recently experienced large increases in induced seismic activity related to wastewater disposal. Although this might imply a lower current potential for induced seismicity than in the mid-continent, the relationship between seismicity and wastewater injection in California has not been fully evaluated. Therefore, the potential level of seismic hazard posed by wastewater disposal is at present uncertain. A comprehensive, in-depth study of spatial and temporal correlations, if any, between wastewater injection and seismicity will be required to provide a firm basis for assessment of seismic hazard related to induced seismicity.

As evidenced by the upswing in induced seismicity in the central and eastern U.S. since 2010, an increase in hydraulic fracturing activity and expanded production in California could increase the seismic hazard from wastewater disposal and perhaps also from hydraulic fracturing, particularly if they involve higher per-well injected volumes approaching those employed elsewhere in the U.S. and a shift to deeper stimulation. However, based on the data presented in Volume I of this study, such shifts in well stimulation in California are not expected in the near or mid term.

The closest wastewater disposal wells to the SAF are located in oilfields just over 10 km (6.2 mi) away in the southern San Joaquin Valley. It is unlikely that current wastewater injection in these wells would induce earthquakes on the fault. If future high-volume injection took place in or close to these existing oilfields, it is plausible that the likelihood of triggering earthquakes on the SAF could increase.

Even if the overall potential for induced seismicity in California proves to be low, some level of incremental seismic hazard and risk assessment to inform permitting and regulation of stimulation-related injection projects is justified. Initial low-level assessment during site screening could be used to place each site into one of a few risk categories, based on planned injection rate, cumulative volume and depth, distance from active or potentially active faults, estimated pressure changes on those faults, background seismicity, and proximity to population centers and critical facilities. An appropriate level of probabilistic seismic hazard and risk assessment would then be carried out for sites in higher risk categories, and the permit would specify bounds on injection parameters to achieve an acceptable level of risk. For these sites, monitoring requirements and operating procedures to manage and, if necessary, mitigate induced seismicity during injections would also be specified.

Injection projects that could possibly cause significant pressure changes on the most active major faults like the SAF should be subject to the most stringent risk assessment and regulatory requirements.

The mechanics of fluid-induced seismicity are fairly well understood, and, as such, it is theoretically possible to carry out full hazard assessments at higher-risk sites. However, much more detailed information on injection than is currently available in publicly available databases will be required, first to gain an understanding of the potential for induced seismicity in California oil-producing basins, and then to carry out hazard and risk assessments. Site-specific investigations will also require definition of local faults, the state of stress on those faults, characterization of rock, fault, and hydrological properties, measurement or modeling of the subsurface pressure perturbation based on injection rates, and characterization of the seismicity at the site and in the surrounding area.

Two aspects of the current DOGGR (2014a) database limit its usefulness in identifying past induced seismicity. First, injected volume rates and wellhead pressures are reported only as (presumed) monthly averages, whereas peak volumes, rates and pressures, and significant short-term variations are of relevance in detecting effects on seismicity. Secondly, depth information is not available for the majority of wastewater injection wells. Filling these gaps in the existing database would facilitate a much more comprehensive analysis of the correlations of injection with seismicity. More complete reporting in the future would enable hazard and risk assessment and mitigation of induced seismicity for new stimulation-related injection operations.

Adequate characterization of local seismicity requires recording of local microearthquakes as small as about M1 or less. Existing regional and local networks provide this detection capability in some areas of California, but the threshold for complete detection in some oil-producing basins is M2 or higher, which presents an obstacle to discriminating potential past induced seismicity in these areas. Moving forward, local microearthquake networks should ideally be installed to monitor seismicity at higher-risk sites located in areas currently having detection thresholds higher than about M1.

The current compilation of stress data for California provides only a sparse sampling of the regional *in situ* field in most areas within oil-producing basins. Therefore, detailed analysis of the potential for induced seismicity and seismic hazard assessment at higher-risk sites would ideally utilize site-specific stress measurements obtained from borehole data and other techniques. Similarly, detecting faults that are potential sources of felt or perhaps damaging induced earthquakes will require site-specific characterization to augment the existing active fault database and geologic maps. Advanced detection of faults on the 100 m to 1 km (328 to 3280 ft) scale that may be sources of small felt earthquakes presents a particular challenge, but these may be revealed by low-magnitude microseismicity during the initial stage of injection.

Inevitably, many of the parameters needed for induced seismicity hazard calculations will be poorly constrained. However, seismic hazard assessment in general is invariably subject to considerable uncertainty, and an important and mature part of the PSHA procedure is to properly characterize the uncertainties in the input parameters, and then propagate them through the calculation to provide rigorous uncertainty bounds on the final hazard estimates.

Induced seismicity that could potentially accompany an increase in well stimulation activity in California could likely be managed and mitigated by adopting a protocol similar to the one developed by the U.S. DOE for enhanced geothermal systems. In addition to hazard and risk assessment, one of the core recommendations in the U.S. DOE protocol is provision of a set of procedures to modify an injection operation in response observed changes in seismicity. These entail staged reduction in injection flow rate and pressure up to and including well shutdown. The procedures should be based on quantitative forecasts of the probability of inducing earthquakes of concern derived from observations of evolving seismicity and changes to the state of the reservoir, rather than the essentially ad hoc criteria that have been employed to date.

4.9. References

Bachmann, C., S. Wiemer, J. Woessner, and S. Hainzl (2011), Statistical Analysis of the Induced Basel 2006 Earthquake Sequence: Introducing a Probability-based Monitoring Approach for Enhanced Geothermal Systems. *Geophys. J. Int.*, 186, 793-807.

Baisch, S., D. Carbon, U. Dannwolf, B. Delacou, M. Devaux, F Dunland, R. Jung, M. Koller, C. Martin, M. Sartori, R. Scenell, and R. Vörös (2009). *Deep Heat Mining Basel Seismic Risk Analysis: SERIANEX*, http://esd.lbl.gov/FILES/research/projects/induced_seismicity/egs/baselfullriskreport.pdf, accessed June 1 2015.

BC Oil and Gas Commission (2012), *Investigation of Observed Seismicity in the Horn River Basin*. Retrieved from http://www.bcogc.ca/node/8046/download, accessed April 30 2015.

Block, L., C. Wood, W. Yeck, and V. King (2014), The 24 January 2013 M_L 4.4 Earthquake near Paradox, Colorado, and its Relation to Deep Well Injection. *Seismol. Res. Let.*, 85, 609-624.

Bommer, J., S. Oates, J. Cepeda, C. Lindholm, J. Bird, R. Torres, G. Marroquin, and J. Rivas (2006), Control of Hazard due to Seismicity Induced by a Hot Fractured Rock Geothermal Project. *Engineering Geology*, 83, 287-306.

Brodsky, E.E., and L.J. Lajoie (2013), Anthropogenic Seismicity Rates and Operational Parameters at the Salton Sea Geothermal Field. *Science, 341*, 543–546, doi:10.1126/science.1239213.

Budnitz, R., G. Apostolakis, D. Boore, L. Cluff, K. Coppersmith, C. Cornell, and P. Morris (1997), *Recommendations for Probabilistic Seismic Hazard Analysis: Guidance on Uncertainty and Use of Experts. NUREG/CR-6372, 170 p*, U.S. Nuclear Regulatory Commission, Washington, DC.

California Geological Survey (1996), http://www.conservation.ca.gov/cgs/rghm/psha/ofr9608/Pages/b_faults4.aspx, accessed April 30, 2015.

Cardno ENTRIX (2012), *Hydraulic Fracturing Study: PXP Ingelwood Oilfield*, Report prepared for Plains Exploration and Production Co. and Los Angeles County Dept. Regional Planning, http://www.ourenergypolicy.org/wp-content/uploads/2012/10/Hydraulic-Fracturing-Study-Inglewood-Field10102012.pdf, accessed April 30 2015.

Cladouhos, T., W. Osborn, et al. (2012), Newberry Volcano EGS Demonstration – Phase I Results. *Proc. 37th Workshop on Geothermal Reservoir Eng.*, Stanford Univ., Jan 30-Feb 1.

Davies, R.J., S.A. Mathias, J. Moss, S. Hustoft, and L. Newport (2012), Hydraulic Fractures: How Far Can They Go? *Mar. Pet. Geol., 37*, 1-6.

Davies, R., G. Foulger, A. Bindley, and P. Styles (2013), Induced Seismicity and Hydraulic Fracturing for the Recovery of Hydrocarbons. *Mar. Pet. Geol., 45*, 171–185.

de Pater, C., and S. Baisch, (2011), *Geomechanical Study of Bowland Shale Seismicity*. StrataGen and Q-con report commissioned by Cuadrilla Resources Limited, UK, 57p.

DOGGR (Division of Oil, Gas and Geothermal Resources) (2010), 2009 Annual Report of the State Oil and Gas Supervisor. *Publication No. PR06*. California Department of Conservation, Sacramento, CA. 267 p.

DOGGR (Division of Oil, Gas and Geothermal Resources) (2014a), "AllWells" shapefile: Geographic Dataset Representing All Oil, Gas, and Geothermal Wells in California Regulated by the Division of Oil, Gas and Geothermal Resources. Updated January 15, 2014. http://www.conservation.ca.gov/dog/maps/Pages/GISMapping2.aspx, last accessed April 30 2015.

DOGGR (Division of Oil, Gas and Geothermal Resources) (2014b), OWRS – Search Oil and Gas Well Records. http://owr.conservation.ca.gov/WellSearch/WellSearch.aspx, last accessed April 30 2015.

Eberhart-Phillips, D., and D.H. Oppenheimer (1984), Induced Seismicity in The Geysers Geothermal Area, California. *J. Geophys. Res., 89*, 1191–1207.

Ekström, G., R. Stein, J. Eaton, and D. Eberhart-Phillips (1992), Seismicity and Geometry of a 110-km-long Blind

Thrust Fault 1. The 1985 Kettleman Hills, California, Earthquake. *J. Geophys. Res. 97*, 4843-4864.

Ellsworth, W.L. (2013), Injection-Induced Earthquakes. *Science, 341*, 142–149. doi: 10.1126/science.1225942.

Fehler M., L. House, W. S. Phillips, and R. Potter (1998), A Method to Allow Temporal Variation in Travel-time Tomography Using Microearthquakes Induced During Hydraulic Fracturing. *Tectonophysics, 289*, 189-201.

Finkbeiner, T., C. Barton, and M. Zoback (1997), Relationships Among In-Situ Stress, Fractures and Faults, and Fluid Flow, Monterey, Formation, Santa Maria Basin, California. *Am. Assoc. Pet. Geol. Bull., 81*, 1975–1999.

Fisher, M., C. Wright, B. Davidson, A. Goodwin, E. Fielder, W. Buckler, and N. Steinsberger (2002), Integrating Fracture-Mapping Technologies To Improve Stimulations in the Barnett Shale. *SPE 77441*, Soc. Pet. Eng. Ann. Tech. Conf., 29 Sep.-2 Oct., San Antonio, TX, 7 p.

Fisher, M., J. Heinze, C. Harris, B. Davidson, C. Wright, and K. Dunn (2004), Optimizing Horizontal Completion Techniques in the Barnett Shale Using Microseismic Fracture Mapping. *SPE-90051*, Soc. Pet. Eng. Ann. Tech. Conf., 26-29 Sep., Houston, TX, 11 p.

Foxall, W., J. Savy, S. Johnson, L. Hutchings, W. Trainor-Guitton, and M. Chen (2013), *Second Generation Toolset for Calculation of Induced Seismicity Risk Profiles*. Report LLNL_TR-634717, Lawrence Livermore Natl. Lab. CA, 24p.

Frohlich, C., E. Potter, C. Hayward, and B. Stump (2010), Dallas-Fort Worth Earthquakes Coincident with Activity Associated with Natural Gas Production. *Leading Edge, 29*, 270-275.

Goebel, T., E. Hauksson, and J-P. Ampuero (2014), A Probabilistic Assessment of Waste Water Injection Induced Seismicity in Central California. *Abstract S51A-4418* presented at the AGU 2014 Fall Meeting, San Francisco, CA, 15-19 Dec.

Hauksson, E., W. Yang, and P. Shearer (2012), Waveform Relocated Earthquake Catalog for Southern California (1981 to 2011). *Bull. Seismol. Soc. Am., 71*, 2239-2244.

Hauksson, E., T. Goebel, E. Cochran, and J-P. Ampuero, (2014) Differentiating Tectonic and Anthropogenic Earthquakes in the Greater Los Angeles Basin, Southern California. *Abstract S51A-4439* presented at the AGU 2014 Fall Meeting, San Francisco, CA, 15-19 Dec.

Healy, J., W. Rubey, D. Griggs, and C. Raleigh (1968), The Denver Earthquakes. *Science, 161*, 1301–1310.

Heidbach, O., Tingay, M., Barth, A., Reinecker, J., Kurfeß, D., and Müller, B. (2008), *The World Stress Map* database release 2008, doi:10.1594/GFZ.WSM.Rel2008.

Herrmann, R., S. Park, and C. Wang (1981), The Denver Earthquakes of 1967-1968. *Bull. Seismol. Soc. Am., 71*, 731–745.

Horton, S. (2012), Disposal of Hydrofracking Waste Fluid by Injection into Subsurface Aquifers Triggers Earthquake Swarm in Central Arkansas with Potential for Damaging Earthquake. *Seismol. Res. Let., 83(2)*, 250–260, doi:10.1785/gssrl.83.2.250.

Hsieh, P.A. and J.D. Bredehoeft, (1981), A Reservoir Analysis of the Denver Earthquakes: A Case Study of Induced Seismicity. *J. Geophys. Res., 86*, 903-920.

Hubbert, M., and W. Rubey (1959), Role of Fluid Pressure in Mechanics of Overthrust Faulting: I. Mechanics of Fluid-filled porous solids and its application to over-thrust faulting. *Bull. Geol. Soc. Am, 70*, 115-166.

Justinic, A.H., B. Stump, C. Hayward, and C. Frohlich (2013), Analysis of the Cleburne, Texas, Earthquake Sequence from June 2009 to June 2010. *Bull. Seismol. Soc. Am., 103*, 3083–3093, doi:10.1785/0120120336.

Kanamori, H., and E. Hauksson (1992), A Slow Earthquake in the Santa Maria Basin, California, *Bull. Seismol. Soc. Am*., 82, 2087-2096.

Kaven, J.O., S. Hickman, and N. Davatzes (2014), Micro-seismicity and Seismic Moment Release within the Coso Geothermal Field, California. *Proc. 39th Workshop on Geothermal Reservoir Eng*., Stanford Univ., Feb. 24-26.

Keller, G.R. and A. Holland (2013). Statement by the Oklahoma Geological Survey, http://www.ogs.ou.edu/earthquakes/OGS_PragueStatement201303.pdf, accessed April 30 2015.

Keranen, K.M., H.M. Savage, G.A. Abers, and E.S. Cochran (2013), Potentially Induced Earthquakes in Oklahoma, USA: Links between Wastewater Injection and the 2011 Mw 5.7 Earthquake Sequence. *Geology, 41*, 699–702, doi:10.1130/G34045.1.

King, V., L. Block, W. Yeck, C. Wood, and S. Derouin (2014), Geological Structure of the Paradox Valley Region, Colorado, and Relationship to Seismicity Induced by Deep Well Injection. *J. Geophys. Res., 119*, doi:10.1002/2013JB010651, 24 p.

Majer, E. L., R. Baria, M. Stark, S. Oates, J. Bommer, B. Smith, and H. Asanuma (2007), Induced Seismicity Associated with Enhanced Geothermal Systems. *Geothermics, 36*, 185–222.

Majer, E, J. Nelson, A. Robertson-Tait, J. Savy, and I. Wong (2012), *A Protocol for Addressing Induced Seismicity Associated with Enhanced Geothermal Systems (EGS)*. DOE/EE Publication 0662, http://esd.lbl.gov/FILES/research/projects/induced_seismicity/egs/EGS-IS-Protocol-Final-Draft-20120124.PDF, accessed April 30 2015.

Majer, E, J. Nelson, A. Robertson-Tait, J. Savy, and I. Wong (2014), *Best Practices for Addressing Induced Seismicity Associated with Enhanced Geothermal Systems (EGS)*. Lawrence Berkeley Natl. Lab. draft report LBNL 6532E, http://esd.lbl.gov/FILES/research/projects/induced_seismicity/egs/Best_Practices_EGS_Induced_Seismicity_Draft_May_23_2013.pdf, accessed April 30 2015.

McGarr, A. (2014), Maximum Magnitude Earthquakes Induced by Fluid Injection. *J. Geophys. Res., 119*, doi:10.1002/2013JB010597, 1008-1019.

McGarr, A., D. Simpson, and L. Seeber (2002), Case Histories of Induced and Triggered Seismicity. In: *International Handbook of Earthquake Engineering and Seismology, Part A*, Eds. W. Lee et al., Academic Press, New York, 933p.

Mena, B., S. Wiemer, and C. Bachmann, (2013), Building Robust Models to Forecast the Induced Seismicity Related to Geothermal Reservoir Enhancement. *Bull. Seismol. Soc. Am., 103*, 383-393.

Murer, A., G. McNeish, T. Urbancic, M. Prince, and A. Baig (2012), Why Monitoring With a Single Downhole Microseismic Array May Not Be Enough: A Case for Multiwell Monitoring of Cyclic Steam in Diatomite. *SPE Reservoir Eval. Eng., 15*, 385-392.

Nicholson, C., and R. Wesson (1990), Earthquake Hazard Associated with Deep Well Injection- A report to the U.S. Environmental Protection Agency. *U.S. Geological Survey Bulletin, v. 1951*, 74p.

NRC (National Research Council) (2013), *Induced Seismicity Potential in Energy Technologies*. The National Academies Press, Washington, D.C.

Rubinstein, J., W. Ellsworth, A. McGarr, and H. Benz (2014), The 2001–Present Induced Earthquake Sequence in the Raton Basin of Northern New Mexico and Southern Colorado. *Bull. Seismol. Soc. Am., 104*, doi 10.1785/0120140009.

Rutledge, J., and S. Phillips (2003), Hydraulic Stimulation of Natural Fractures as Revealed by Induced Microearthquakes, Carthage Cotton Valley Gas Field, East Texas. *Geophysics, 68*, 441-452.

Shapiro, S. A., R. Patzig, E. Rothert, J. Rindschwentner (2003), Triggering of Seismicity by Pore-pressure Perturbations: Permeability-related Signatures of the phenomenon. Pure App. *Geophys. 160*, 1051-1066.

Shapiro, S.A., C. Dinske, and J. Kummerow (2007), Probability of a Given-magnitude Earthquake Induced by Fluid Injection. *Geophys. Res. Let., 34*, doi:10.1029/2007GL031615.

Shapiro, S. A. and C. Dinske (2009), Scaling of Seismicity by Nonlinear Fluid-rock Interaction. *J. Geophys. Res., 114*, doi:10.1029/2009JB006145.

Shapiro, S. A., Krüger, O. S., Dinske, C., and Langenbruch, C. (2011), Magnitudes of induced earthquakes and geometric scales of fluid-stimulated rock volumes. *Geophysics, 76*(6), WC55-WC63.

Shemeta, J., W. Minner, R. Hickman, P. Johnston, C. Wright, and N. Watchi (1994), Geophysical Monitoring During a Hydraulic Fracture in a Fractured Reservoir: Tiltmeter and Passive Seismic Results. In: *Eurorock '94*, Delft, Netherlands. Balkema, Rotterdam, 929-944.

Sumy, D., E. Cochran, K. Keranen, M. Wei, and G. Abers (2014), Observations of Static Coulomb Stress Triggering of the November 2011 M5.7 Oklahoma Earthquake Sequence. *J. Geophys. Res. 119*, 1–20, doi:10.1002/2013JB010612.

Townend, J., and M.D. Zoback (2000), How Faulting Keeps the Crust Strong. *Geology, 28*, 399–402. doi:10.1130/0091-7613(2000), 28-399.

U.S. Geological Survey (1990), *The Coalinga, California, Earthquake of May 2, 1983*. USGS Professional Paper 1487, 417 p.

U.S. Geological Survey (2015), http://earthquake.usgs.gov/research/induced, accessed April 30, 2015.

Weingarten, M., and S. Ge (2014), Is High-rate Injection Causing the Increase in U.S. Mid-continent Seismicity? *Abstract S54A-03* presented at the AGU 2014 Fall Meeting, San Francisco, CA, 15-19 Dec.

Wiemer, S. and M. Wyss (2000), Minimum Magnitude of Complete Reporting in Earthquake Catalogs: Examples from Alaska, the Western United States, and Japan. Bull. *Seismol. Soc. Am., 90*, 859-869.

Zoback, M. (2012), Managing the Seismic Risk Posed by Wastewater Disposal. *EARTH Magazine, April*, 38-43.